Czech Technical University in Prague
Faculty of Electrical Engineering
Department of Control Engineering

Active control for high capacity flexible aircraft

DOCTORAL THESIS

January 2012 Ing. Tomáš Haniš

Czech Technical University in Prague
Faculty of Electrical Engineering
Department of Control Engineering

Active control for high capacity flexible aircraft

by

Ing. Tomáš Haniš

Supervisor: Ing. Martin Hromčík, Ph.D.

Dissertation submitted to the Faculty of Electrical Engineering of
Czech Technical University in Prague
in partial fulfillment of the requirements
for the degree of

Doctor

in the branch of study
Control Engineering and Robotics
of study program Electrical Engineering and Informatics

January 2012

To my family.

Preface

The efficient algorithms for flexible aircraft control design is presented in this research work. The novel approach of non-convex optimization is extensively used to provide low order control system for Blended Wing Body type aircraft with considerably flexible structure. The attention is paid to design feedback as well as feed-forward control system providing required handling qualities and simultaneously structure load attenuation.

I started my work on aircraft control systems as a MSc. student when I became a member of a research team lead by Dr. Martin Hromčík from the Czech Technical University in Prague, whose major research domains are optimal control systems with application in aerospace and development of polynomial methods for control and filter design. I joined the European project "Active Control for Flexible Aircraft 2020" that was just starting at that time. I had the opportunity to get involved in the research team, gradually absorb the knowledge cultivated in this world leading group, and, finally, contribute to further development of the field by proposing routines for various optimization and control tasks.

Thanks to fruitful discussions and mutual interactions with other members of the team, mainly with Andreas Wildschek (EADS IW, Munich, Germany), Alexander Schirrer, Christian Westermayer, Mark Hemedi and Martin Kozek (TUW, Vienna, Austria) new ideas on aircraft control design raised. We developed an algorithms for the Control Augmentation System and feed-forward Load Alleviation System.

First and foremost, I would like to express my gratitude to my supervisor Martin Hromčík for giving me an opportunity to join his research team, for creating perfect conditions for my research, for encouragement and motivation and for introducing me to the world of research.

I also wish to thank my colleagues at the Department of Control Engineering at Czech Technical University in Prague, especially to Jan Rathousky, Martin Řezáč, Zdeněk Hurák, Jana Nováková and Pavel Hospodář, for creating enjoyable and inspiring environment.

My deepest obligation comes to my parents for bringing me up and supporting during studies. I also wish to thank my friends Láda Bušta, Jirka Hanzlík, Hynek

Frauenberg, Jan Benda, Tomáš Dort and Zuzana Novotná for keeping my mind relaxed.

Concerning the financial arrangements, this work was supported by European project ACFA2020 and the Ministry of Education of the Czech Republic under Project No. 213321. In addition, crucial business trips to major international conferences, where the results summarized in this thesis were presented and discussed with leading world experts in the field, could be undertaken thanks to the Travel Grants kindly provided by the foundation "Nadání Josefa, Marie a Zdeňky Hlávkových" (http://www.hlavkovanadace.cz).

Tomáš Haniš

Czech Technical University in Prague
Prague, January 2012

Active control for high capacity flexible aircraft

Ing. Tomáš Haniš

Czech Technical University in Prague, Prague, January 2012

Supervisor: Ing. Martin Hromčík, Ph.D.

This thesis is devoted to design of algorithms for flexible aircraft control systems. The Blended Wing Body type aircraft is addressed to present methodology results. A new approach to optimal placement of sensors (OSP) in mechanical structures is presented. In contrast to existing methods, the presented procedure enables a designer to seek for a trade-off between the presence of desirable modes in captured measurements, and the elimination of influence of those mode shapes that are not of interest in a given situation. An efficient numerical algorithm is presented, developed from an existing routine based on the Fischer information matrix analysis. We consider two requirements in the optimal sensor placement procedure. On top of the classical EFI approach, the sensors configuration should also minimize spillover of unwanted higher modes. We use the information approach to OSP, based on the effective independent method (EFI), and modify the underlying criterion to meet both of our requirements - to maximize useful signals and minimize spillover of unwanted modes at the same time. The results of sensor optimization are directly used for robust feedback control. Advanced non-convex non-smooth optimization techniques for fixed-order H infinity robust control are proposed to design of flight control systems (FCS) with prescribed structure. Compared to classical techniques - tuning of and successive closures of particular single-input single-output (SISO) loops like dampers, attitude stabilizers etc. - all loops are designed simultaneously by means of quite intuitive weighting filters selection. In contrast to standard optimization techniques, though (H_2, H_∞ optimization), the resulting controller respects the prescribed structure in terms of engaged channels and orders (e.g. P, PI, PID controllers). In addition, robustness w.r.t. multi model

uncertainty is also addressed which is of most importance for aerospace applications as well. Such a way, robust controllers for various Mach numbers, altitudes, or mass cases can be obtained directly, based only on particular mathematical models for respective combinations of the flight parameters.

Contents

List of Figures

Chapter 1

Introduction

1.1 Motivation

This thesis is closely related to ACFA 2020 collaborative research project funded by the European Commission under the seventh research framework programme (FP7). The ACFA 2020 project deals with innovative active control concepts for ultra efficient 2020 aircraft configurations like the blended wing body (BWB) aircraft (see 1.1). The Advisory Council for Aeronautics Research in Europe (ACARE) formulated the "ACARE vision 2020", which aims for 50% reduced fuel consumption and related CO_2 emissions per passenger-kilometre and reduction of external noise. To meet these goals is very important to minimize the environmental impact of air traffic but also of vital interest for the aircraft industry to enable future growth. Blended Wing Body type aircraft configurations are seen as the most promising future concept to fulfill the ACARE vision 2020 goals because aircraft efficiency can be dramatically increased through minimization of the wetted area and reducing of structural load and vibration by active damping in a integrated control law design (addopted from www.acfa2020.eu).

Figure 1.1: BWB visualization.

Partners involved in ACFA 2020 project:

- EADS Innovation Works
- Airbus France
- Alenia Aeronautica S.p.A.
- HELLENIC AEROSPACE INDUSTRY S.A.
- Israel Aerospace Industries
- Deutsches Zentrum für Luft- und Raumfahrt e.V.
- ONERA
- FOI, Swedish Defense Research Agency
- Technical University Munich
- Vienna University of Technology
- Institute of Mechanics and Mechatronics
- Czech Technical University
- National Technical University Athens

- Bialystok Technical University

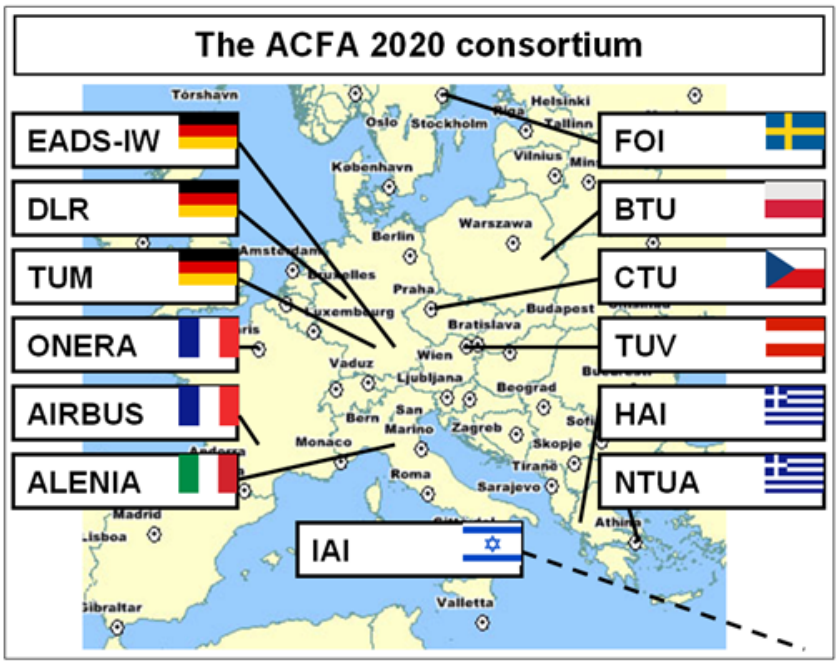

Figure 1.2: ACFA 2020 partners.

1.2 State of the Art

A nice overview and literature survey of Blended Wing Body type aircrafts and optimal control designs at aerospace have been recently done in the Ph.D. theses of my colleagues Alexander Schirrer (Schirrer, November 2011), Christian Westermayer (Westermayer, November 2011) and Mark Hemedi from Technical University in Vienna (Vienna, Austria). The sections 1.2.1 and 1.2.2 are therefore adopted to a great extend from the work of Christian Westermayer (Westermayer, November 2011).

1.2.1 Blended wing body aircraft concepts (BWB)

A comprehensive documentation of US research effort on the design of BWB subsonic transport aircraft, corresponding design issues and constraints, advantages and drawbacks given by such configuration, as well as results from wind-tunnel tests are presented in (Liebeck, 2004). Thereby, the research progress is demonstrated starting from a preliminary design study in 1988 for novel configurations up to the highly efficient Boeing BWB-450 baseline aircraft. Basically, three generations of BWB configurations are documented which were successively improved. Starting from the design requirements definition, the disciplines aerodynamics, structure, stability and control, propulsion, and performance are discussed. Thereby, the importance of the shape of the airfoil for the center body and the outer wings for longitudinal static stability as well as aerodynamic performance is clearly outlined. Moreover, the attainable benefits in structural loads are shown in comparison to conventional configurations. Additionally, the overall performance improvement in terms of fuel burn per seat mile is denoted as 27%.

A detailed aerodynamic analysis of a BWB configuration is considered in the European project MOB and relevant results are presented in (Qin et al., 2004). Therein, starting from a baseline configuration, the effects of different spanwise loading distributions, sectional airfoil profile adaptation, local twist variation and three dimensional shaping are investigated and the effects on aerodynamic performance concerning lift to drag ratio are determined. A noticeable outcome from this study is that a triangular-elliptic spanwise lift distribution outperforms the elliptic distribution. At the same time it is important to find a trade-off between induced drag and wave drag for optimized aerodynamic performance. Finally, the relevance of a multidisciplinary design optimization (MDO) is emphasized in order to maximize overall aircraft performance.

The preliminary multi-disciplinary design optimization for a BWB configuration is the topic of (Hansen et al., 2006). In this work, a numerical design tool is presented which was adapted to the needs of this unconventional configuration in order to provide meaningful results. Various structural solutions for a 700 passenger BWB aircraft are obtained with special emphasis on the design disciplines geometry, aerodynamics, propulsion, flight mission requirements, structural siz-

ing, and component mass. For load prediction, both manoeuvre loads as well as gust loads are evaluated at different aircraft mass and center of gravity positions. Finally, the effectiveness of the design tool is demonstrated based on the design of three BWB configurations, where the same design requirements were assumed, however, the number of ribs in the fuselage differs. A tool for the generation of a nonlinear flight mechanics model of a BWB configuration within the MDO process is presented in (Voskuijl et al., 2008). The aim of this tool is to evaluate the rigid body dynamical behavior of the aircraft as well as the effectiveness of various control surface locations in an early design phase. While in this work only a rigid body aircraft model is considered, the necessity for a more complex, coupled aeroelastic model is discussed.

1.2.2 Aircraft robust control design

The topic of aeroelastic modeling, that is the development of an integrated aircraft model containing flight mechanics, aeroelastics as well as their coupling is treated in detail in (Schuler, 1997). In this work the modeling process for a large flexible transport aircraft is presented, with special emphasis on the structural dynamics, related steady and unsteady aerodynamics and their coupling with the rigid body dynamics. Moreover, a detailed system analysis is provided and relevant aspects for further control design are discussed. Finally, a H_∞ robust aeroelasti control design approach based on a multi-model, multi-criteria onset using three selected operating points is presented. Thereby, design goals of a typical stability augmentation system and an aeroelastic control system are considered in an integrated manner and the main results are outlined.

The process of generating an integrated aeroelastic model for a transport aircraft and subsequent robust controller design is also presented in (Hanel, 2001). At the beginning, the subsequent modeling steps are outlined in detail under consideration of numerical issues, model complexity and attainable model accuracy. Furthermore, the sensor placement task for flexible aircraft control is discussed. The main part is dedicated to the design of an integrated robust flight and aeroelastic controller. The design requirements such as stability augmentation and active aeroelastic damping are treated jointly over a large operating region. Therefore,

a unification of low frequency flight dynamics is achieved by gain scheduled inner loops using relevant flight mechanic data. Based on such modified models, robust H_∞ controllers for longitudinal and lateral motion are designed using μ-synthesis. Good results are achieved in linear and nonlinear simulations concerning handling qualities and reduction of aeroelastic vibrations. A μ-synthesis approach for longitudinal motion of a B-52 is also shown in (Aouf et al., 2000). In this work, the reduction in vertical accelerations caused by turbulence gust is the main goal, whereas disturbances are simulated using a Dryden gust model. The tuning process is outlined as well as a comparison to results from H_∞ optimization are provided.

The aforementioned references (Schuler, 1997), (Hanel, 2001), (Aouf et al., 2000) all used the H_∞-methodology for robust controller design. The topic of robust multi-input multi-output (MIMO) feedback control in general using the H_∞-methodology is shown in a textbook (Skogestad and Postlethwaite, 2005). In this book the fundamentals of uncertainty modeling, robust stability and performance analysis, and robust controller design for MIMO systems is described. Moreover, general limitations for MIMO control, the selection of the control structure, and system reduction techniques are outlined. Based on several case studies, the entire design process of H_∞ robust controllers is illustrated.

1.3 Outline of thesis

The immediately following, second chapter, gives the specific goals and objectives of this dissertation. Particular items are then developed in further chapters.

The third chapter contains the first major contribution of the thesis: an Optimal Sensors Placement methodology focusing on higher modes spillover minimization.

In the fourth chapter, two robust feedback control systems of low complexity are introduced. First one is fully integrated lateral control system (aircraft rigid body motion as well as flexible modes are controlled by one control system of low order). Second, the longitudinal rigid body motion Control Augmentation System constrained by prescribed structure is delivered.

The fifth chapter deals with feed-forward Gust Load Alleviation System (GLAS)

designed by convex optimization technique.

The sixth chapter summarizes the scientific achievements of this thesis and outlines immediate opportunities for improvement and further research.

In the seventh chapter, the results of the thesis are summed up and confronted with the goals and objectives set in chapter 2.

Chapter 8 contains the publications of the authors, related directly and indirectly to the thesis, and other references used throughout the text.

Chapter 2

Goals and Objectives of the Disertation

Specific goals of this dissertation were set as follows:

1. Develop methodology for optimal sensor placement based on mathematical model of flexible aircraft structure. The results of this optimization task will be later on used in this thesis as a recommendation for aircraft structural control system measurements.

   Existing aircraft control system concepts either do not consider aircraft structure flexibility, or selection of suitable measurements is based on designers experience.

2. Deliver robust feedback control system design methodology for aircraft with flexible structure based on modern optimization techniques. The resulting control system should address both aircraft rigid body control (Control Augmentation system) and aircraft flexible structure control. Modularity of such a control system as well as low complexity is required.

   Existing methodologies are based on hierarchical control designs (mostly P or PI controllers), or H_2 optimization techniques like LQ controller and usually address just rigid body motion of aircraft.

3. Design feed-forward load alleviation control system for aircraft with flexible structure. It is important to reduce structural load in order to bring structural mass saving and still preserve aircraft lifetime.

Chapter 3

Optimal sensors placement and spillover suppression

A new approach to optimal placement of sensors (OSP) in mechanical structures is presented. In contrast to existing methods, the presented procedure enables a designer to seek for a trade-off between the presence of desirable modes in captured measurements, and the elimination of influence of those mode shapes that are not of interest in a given situation. An efficient numerical algorithm is presented, developed from an existing routine based on the Fischer information matrix analysis. Two requirements are considered in the optimal sensor placement procedure. On top of the classical EFI approach, the sensors configuration should also minimize spillover of unwanted higher modes. The information approach is used to OSP, based on the effective independent method (EFI), and modify the underlying criterion to meet both of our requirements - to maximize useful signals and minimize spillover of unwanted modes at the same time. Performance of presented approach is demonstrated by means of examples, and a flexible Blended Wing Body (BWB) aircraft case study related to a running European-level FP7 research project 'ACFA 2020 - Active Control for Flexible Aircraft'.

3.1 Introduction

Optimal sensor placement (OSP) in mechanical systems and structures has become a popular and frequently discussed research topic during last ten years. Applications cover modeling, identification, fault detection, and active control of such systems as bridges (Meo and Zumpano, 2005) (Li et al., 2007), rail wagons (Benatzky et al., 2008), large space structures (Yao et al., 1992). The goal is to tell the designers of the whole mechanical system where displacement, force, inertial acceleration, or other sensors are to be installed so that they are as informative as possible.

Various approaches have been developed. We will mention two in brief. The former, information based approach, is based on the analysis of the output shape matrix. An iterative elimination algorithm, denoted as EFI (for "Effective Independence") has been developed that repeatedly deletes the lines of the initial, full output shape matrix with lowest amount of information, measured by either the trace or determinant of an underlying Fischer information matrix. See (Kammer, 1991) for more detailed treatments and (Meo and Zumpano, 2005) (Li et al., 2007) (Yao et al., 1992) for some case studies.

An alternative approach is based on the idea of maximizing the energy of the underlying modes in the optimally placed sensors. Related procedures lead to optimization problems over output Gramians of the system. References: (Gawronski, 2004).

Both these approaches are applied on pre-selected modes of interest. For instance, in an active damping application for a transport vehicle, see a recent report (Benatzky et al., 2008), the bandwidth and thus implied modes are defined according to some comfort standards and considerations regarding impact of particular modes on the loads induced in the structure. Typically, a few lower modes are selected as a result of such analysis. Resulting optimal sensors selection is subsequently called, with only those pre-selected modes in mind.

However, also those not-considered, typically mid- or high-frequency modes are still present in the process and, if excited by disturbances or the control action, they can influence the active damping system behavior in an unexpected manner. This phenomenon, denoted as spillover, cannot be captured directly by the two existing

approaches mentioned above. Although some procedures have been developed that address these issues, see e.g. (Kim and Inman, 2001), they are based on advanced signal processing (filtering) of the measured signals and do not suggest how to modify the sensors positions themselves accordingly.

And it is exactly the problem that this paper is focused on. The aforementioned information approach is taken as the starting point. The underlying criterion is modified so that the influence of desirable modes is maximized, and those unwanted modes are minimized in the observations at the same time, see section 3.2. The result is a compromise where suitably chosen simple weights serve as a tuning knob for the designer. A related numerical procedure is then developed, based on the EFI approach, in section 3.3. Two examples are presented in section 3.4 where one can appreciate the intuitively expected placements and study the influence of tuning. Further, a case study related to a large flexible BWB aircraft and its active vibration control system is presented in section 3.5.

3.2 The effective independence method (EFI)

Optimal sensors placement techniques are extensively discussed in papers (Kammer, 1991) (Kammer, 1995) (Kammer, 1992) (Kammer and Tinker, 2004) (Kammer, 2005) (Poston and Tolson, 1992) (Meo and Zumpano, 2005) (Li et al., 2007). A short overview of the EFI method follows in this section 3.2, adopted from (Meo and Zumpano, 2005) (Li et al., 2007).

The aim of the EFI method is to select measurement positions that make the mode shapes readings of interest as linearly independent as possible. The method originates from the estimation theory and is based on maximization of related Fisher information matrix, measured by its determinant or trace. That is in fact equivalent to minimization of the condition number of the information matrix related to selected sensors. The number of sensors is iteratively reduced from an initially large candidate set by removing those sensors which contribute least of all the candidate position to the linear independence of the target modes readings. In the end, the remaining sensors are delivered as the optimal sensor set. As a useful guideline to stop the iterative removing process, the determinant of the Fisher information matrix can be plotted with respect to the number of sensors; if

a considerable drop is identified, further reduction should be considered with care.

3.2.1 Structural model

The sensor placement problem can be investigated from uncoupled modal coordinates of governing structural equations as follows:

$$\ddot{q}_i + M_i^{-1} \cdot C_i \cdot \dot{q}_i + M_i^{-1} \cdot K_i \cdot q_i = M_i^{-1} \cdot \Phi_i^T \cdot B_0 \cdot u \tag{3.1}$$

$$y = \Phi \cdot q + \epsilon = \sum_{i=1}^{N} q_i \cdot \Phi_i + \epsilon \tag{3.2}$$

where q_i is the i^{th} modal coordinate and is also the i^{th} element of the vector, q, in the 2^{nd} equation, M_i, K_i and C_i are the corresponding i^{th} modal mass, stiffness and damping matrix, respectively, Φ is the mode shape matrix with its i^{th} column as the i^{th} mass-normalized mode shape, B_0 is simply a location matrix formed by ones (corresponding to actuators) and zeros (no load), specifying the positions of the force vector u. y is a measurement column vector indicating which positions of the structure are measured, and ϵ is a stationary Gaussian white noise with zero mean and a variance of σ^2.

3.2.2 Method principle

From the output measurement, the EFI algorithm analyzes the covariance matrix of the estimate error for an efficient unbiased estimate of the modal coordinates as follows (Kammer, 1995) (Kammer, 1992) (Kammer and Tinker, 2004) (Kammer, 2005) (Poston and Tolson, 1992) (Meo and Zumpano, 2005):

$$\begin{gathered} E\left[(q-\hat{q}) \cdot (q-\hat{q})^T\right] = \\ \left[\left(\frac{\partial y}{\partial q}\right)^T \cdot \left[\sigma^2\right]^{-1} \cdot \left(\frac{\partial y}{\partial q}\right)\right]^{-1} = Q^{-1} \end{gathered} \tag{3.3}$$

where Q is the Fisher information matrix, σ^2 represents the variance of the stationary Gaussian measurement white noise ϵ in (3.2), E denote the mean value,

and $\hat{q}$ is the efficient unbiased estimate of q. Maximizing Q over all sensors positions will result in the best state estimate of q. Ψ denotes the eigenvectors matrix of Q and λ is related diagonal eigenvalue matrix. The EFI coefficients of the candidate sensors are computed by the following formula:

$$E_D = [\Phi \cdot \Psi] \otimes [\Phi \cdot \Psi] \cdot \lambda^{-1} \cdot 1 \tag{3.4}$$

where $\otimes$ represents a term-by-term matrix multiplication, and $\mathbf{1}$ is an $n \times 1$ column vector with all elements of $\mathbf{1}$. E_D's entries are the EFI indices, which evaluate the contribution of all candidate sensor locations to the linear independence of the target modes measurement. Simple selection procedure is then employed to sort the elements of the E_D vector, and to remove its smallest entry at a time and also related candidate sensor, giving rise to a reduced mode shape matrix Φ. The E_D coefficients are then updated according to the new modal shape matrix, and the process is repeated iteratively until the number of remaining sensors equals a preset value. The remaining lines of the Φ matrix (or related EFI indices) define the optimal measurement locations.

3.3 The effective independence method with modified criterion

The main result of the paper is presented in this section. We develop a numerical scheme for OSP, based on the EFI method, such that the spillover (Liu et al., 2006) (Choi and Park, 2001) (Chait and Radcliffet, 1989) (Choi and Park, 1989) of unwanted higher modes is minimized.

3.3.1 Method principle

The modified criterion is based on the EFI reasoning presented above. Main task of the pure EFI is just to maximize information on desired modes through optimal configuration of sensors (measurements) expressed by the Fisher information matrix (FIM), or its trace or determinant respectively. The modified criterion we propose reads:

$$J_{MEFI} = \alpha J_{EFI} + (1-\alpha) J_{SNR} \tag{3.5}$$

with optimum

$$J^*_{MEFI}(\alpha_0) = max_{\substack{[i,j,k]\in\Omega \\ \alpha=\alpha_0}} [\alpha J_{EFI} + (1-\alpha) J_{SNR}] \tag{3.6}$$

where

$$J_{EFI} = trace\left(Q^m_{[i,j,k]}\right) \tag{3.7}$$

with optimum

$$J^*_{EFI} = max_{[i,j,k]\in\Omega} trace\left(Q^m_{[i,j,k]}\right) \tag{3.8}$$

stands for the standard EFI part (maximize the information content for those desirable modes), and

$$J_{SNR} = \frac{trace\left(Q^m_{[i,j,k]}\right)}{trace\left(Q^n_{[i,j,k]}\right)} \tag{3.9}$$

with optimum

$$J^*_{SNR} = max_{[i,j,k]\in\Omega} \left[\frac{trace\left(Q^m_{[i,j,k]}\right)}{trace\left(Q^n_{[i,j,k]}\right)}\right] \tag{3.10}$$

is a newly added term to penalize the unwanted mode shapes in sensors readings. Ω is the set of all candidate triples of sensors (we are considering three sensors to be selected to simplify indexing). $Q^m_{[i,j,k]}$ is the Fisher information matrix (see (3.3)) for m^{th} modes (those to be captured), where $Q^n_{[i,j,k]}$ is the Fisher information matrix for the unwanted modes. Note that maximizing (3.9) increases information about the desirable modes in the measurements (maximizing numerator of (3.9) and simultaneously suppresses the unwanted modes influence (minimizing denominator of (3.9).

The coefficient $\alpha \in (0,1)$ serves as a tuning parameter and defines the relative importance of each part of the criterion. Selection of the parameter α is problem-dependent. However, although it is not possible to give a generally valid value for α, its influence for particular data can be investigated by means of related SNR-plots as explained in Example 1 in detail, see section 3.4).

The ratio part in J_{SNR} however becomes problematic as both terms in $\frac{trace\left(Q^m_{[i,j,k]}\right)}{trace\left(Q^n_{[i,j,k]}\right)}$ approach zero (near the nodes of both desirable and unwanted mode shapes) which leads to irrelevant results. This unintended behavior is suppressed by applying a suitable mapping function on $trace\left(Q^m_{[i,j,k]}\right)$ and $trace\left(Q^n_{[i,j,k]}\right)$ to assure for reasonably high information content (those degenerated, almost $\frac{0}{0}$ candidates, are effectively discriminated). A suitable mapping function can take the following form, for example (see also Fig. 3.1):

$$f(t) = \sqrt[n]{(1+t^n)}. \tag{3.11}$$

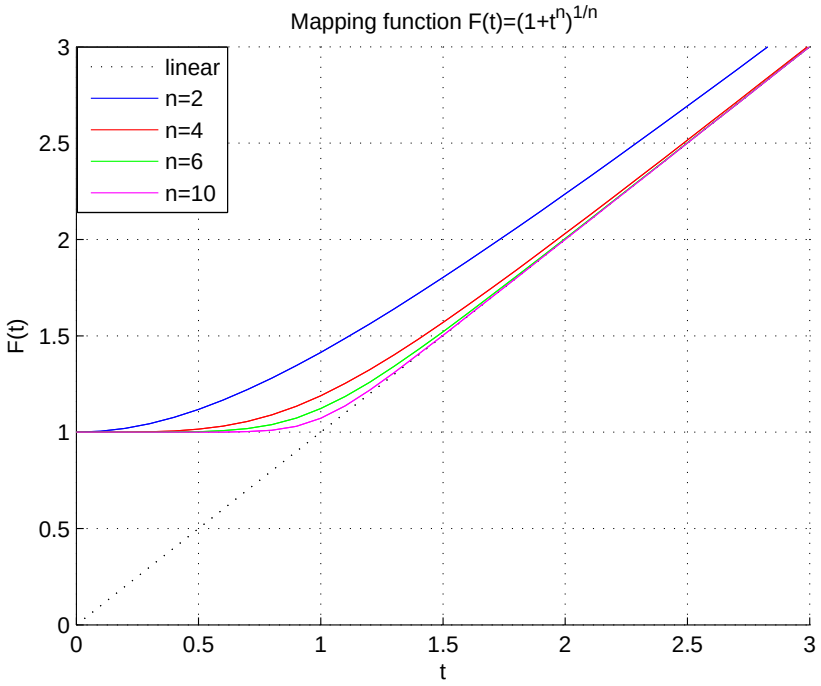

Figure 3.1: Mapping function.

3.3.2 Modified EFI algorithm

Now we have an accordingly modified criterion. Next task is to modify the EFI heuristic in a very similar manner, to arrive at a tractable numerical scheme for the problem. Critical part of EFI method is in evaluation of E_D vector (see (3.4)), so the modified evaluation takes the following shape:

$$\begin{aligned} E_{DM}(\alpha) &= \alpha E_D + (1-\alpha) E_{DSNR} \\ E_D &= [\Phi \cdot \Psi] \otimes [\Phi \cdot \Psi] \cdot \lambda^{-1} \cdot 1 \\ E_{DSNR} &= \frac{[\Phi^m \cdot \Psi^m] \otimes [\Phi^m \cdot \Psi^m] \cdot \lambda^{m-1} \cdot 1}{[\Phi^n \cdot \Psi^n] \otimes [\Phi^n \cdot \Psi^n] \cdot \lambda^{n-1} \cdot 1}. \end{aligned} \tag{3.12}$$

Note that potential numerical issues near the nodes points are covered by the mapping function (3.11) applied on E_D and E_{DSNR} vector.

3.4 Example

Let us consider a flexible system with two modes of intrest depicted in Fig. 3.2. Its structural equations read

$$\begin{bmatrix} 1 & 0 \\ 0 & 1 \end{bmatrix} \cdot \ddot{q} + \begin{bmatrix} 0.1 & 0 \\ 0 & 0.1 \end{bmatrix} \cdot \dot{q} + \begin{bmatrix} 0.1 & 0 \\ 0 & 0.1 \end{bmatrix} \cdot q = \Phi^T \cdot I_{33x33} \cdot u \tag{3.13}$$

$$y = \Phi \cdot q \tag{3.14}$$

$$\Phi^T = [\begin{matrix} 0 & 0.0998 & 0.1987 & 0.2955 & 0.3894 & 0.4794 & 0.5646 & 0.6442 & ... \\ 0 & 0.0000 & 0.0000 & 0.0000 & 0.0001 & 0.0006 & 0.0033 & 0.0123 & ... \end{matrix}$$

$$\begin{matrix} 0.7174 & 0.7833 & 0.8415 & 0.8912 & 0.9320 & 0.9636 & 0.9854 & 0.9975 & ... \\ 0.0361 & 0.0870 & 0.1780 & 0.3161 & 0.4947 & 0.6899 & 0.8637 & 0.9752 & ... \end{matrix}$$

$$\begin{matrix} 0.9996 & 0.9917 & 0.9738 & 0.9463 & 0.9093 & 0.8632 & 0.8085 & 0.7457 & ... \\ 0.9957 & 0.9197 & 0.7672 & 0.5758 & 0.3864 & 0.2297 & 0.1193 & 0.0532 & ... \end{matrix}$$

$$\begin{matrix} 0.6755 & 0.5985 & 0.5155 & 0.4274 & 0.3350 & 0.2392 & 0.1411 & 0.0416 \\ 0.0198 & 0.0059 & 0.0013 & 0.0002 & 0.0000 & 0.0000 & 0.0000 & 0.0000 \end{matrix}].$$

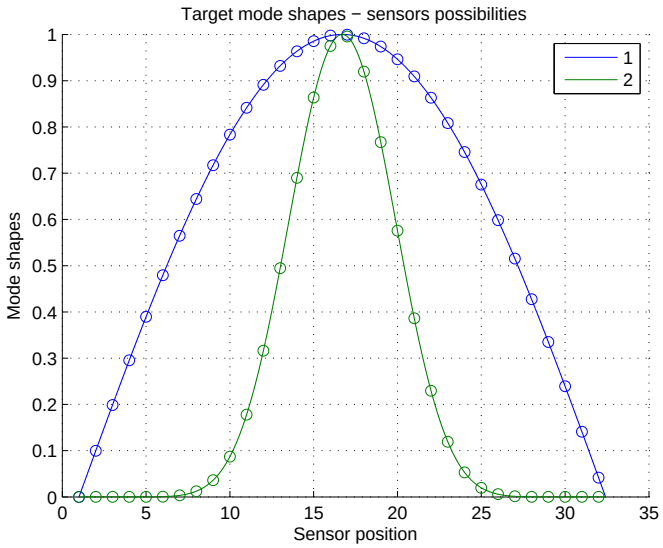

Figure 3.2: Mode shapes and candidate sensor positions.

In this case it is fairly intuitive to decide by common sense where sensors should be placed if we want to maximize measurement of the first mode and reduce the second one. One can see results of the classical EFI approach in Fig. 3.6, related to the EFI criterion (3.7). It is clear that the EFI approach gives rise to sensors configuration optimal to fit the desired mode (first one), but spillover of the second one is huge. Measured energy of both modes (required E_{RQ} and not required E_{NOTRQ}) is printed in upward Fig. 3.6. The signal to noise ratio coefficient (defined in dB units) was evaluated to represent spillover. SNR is defined by following form:

$$SNR = 20 \cdot log_{10} \left(\frac{E_{RQ}}{E_{NOTRQ}} \right). \tag{3.15}$$

Spillover reduction of the unwanted mode can be achieved by our modified criterion (see 3.5). First, one has to select the α-value properly in the modified criterion (3.5). The dependencies of the captured energy of wanted modes (E_{RQ}) and of the captured energy of unwanted modes (E_{NOTRQ}) on α are depicted in

Fig. 3.3. The optimal selection of the α value is at the point where E_{RQ} is large and E_{NOTRQ} is still sufficiently small. In our case, the suitable range for α is apparently the 0.2-0.3 interval, and the value of 0.25 is therefore selected.

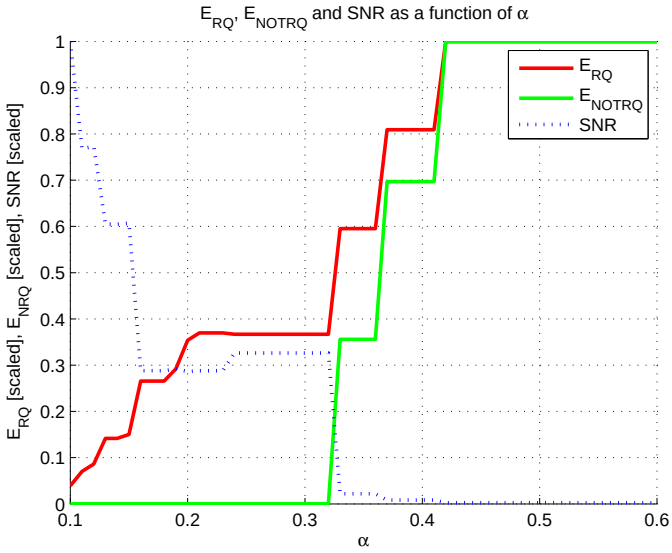

Figure 3.3: The α-dependency of SNR coefficient, captured energy of required(J_{RQ}) and not required(J_{NOTRQ}) modes.

Having α, we can proceed with the modified criterion (3.5) and related modified EFI algorithm of the section 3.3.2. Results are presented in Fig. 3.4. One can see that spillover of the second mode with respect to the first mode is reduced if the sensors are selected according to the proposed criterion (3.5), and that the measurement of the useful mode is still at a good level. In addition, the suggested modified EFI algorithm appears to be an efficient approach to solve the problem (3.5) - mind the modes symmetry and compare (3.4) (modified EFI algorithm) and Fig. 3.5 (optimum of (3.5) found by "brute force" - in this particular very simple case it is feasible to exploit all the sensors combinations and select the true optimum, at the cost of high computational burden though).

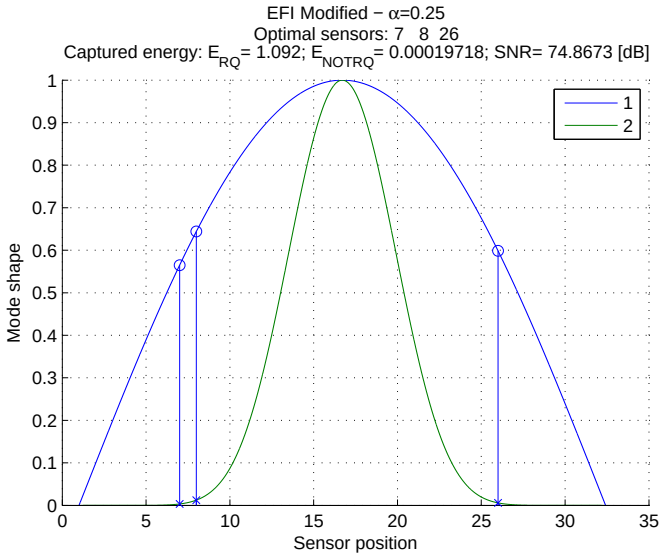

Figure 3.4: OSP by the modified EFI algorithm.

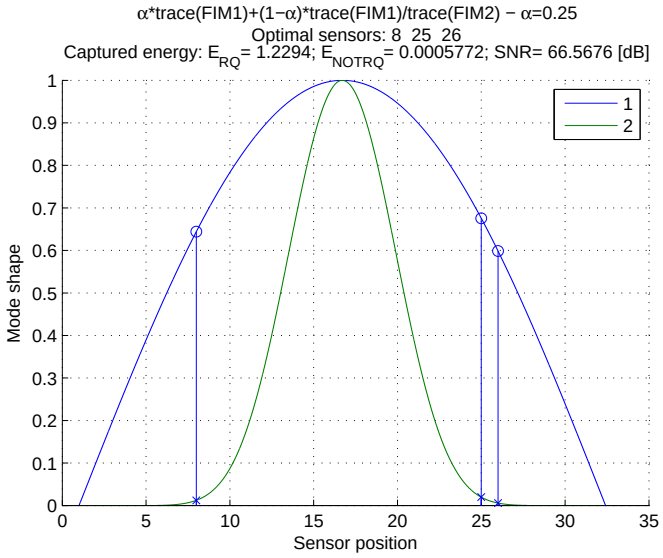

Figure 3.5: OSP by direct maximization of J_{MEFI}.

For completeness, the standard EFI approach results for three sensors are given in Fig. 3.6. Obviously, 1^{st} mode is captured very well (which is good), nevertheless, the 2^{nd} mode is not attenuated at all (it is not a part of the problem formulation

for the standard EFI approach).

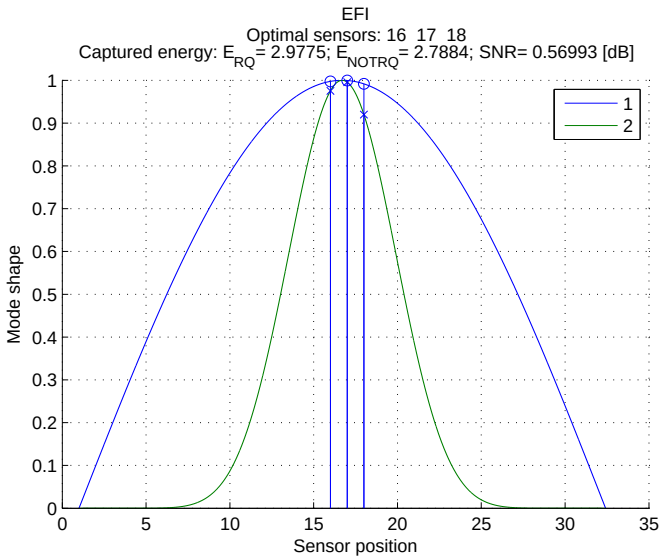

Figure 3.6: OSP by classical EFI.

3.5 Case study

The ability to distinguish between particular modes in measurement simply by optimization of appropriate sensor configuration is critical in this application due to presence of more flexible modes in a narrow frequency range of 0-10 Hz. We cannot therefore rely on signal processing (filtering), and we have to think of a smart sensors configuration instead.

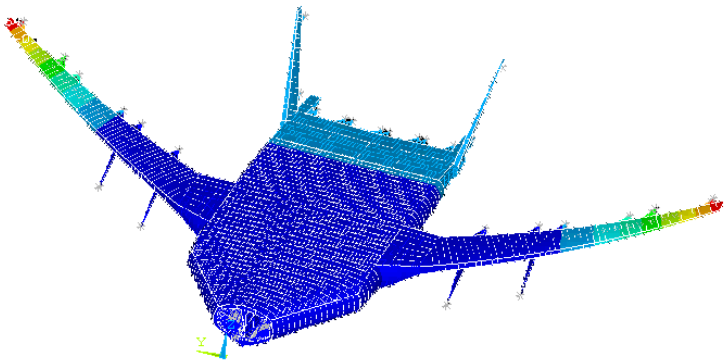

Figure 3.7: Shape of 1^{st} mode.

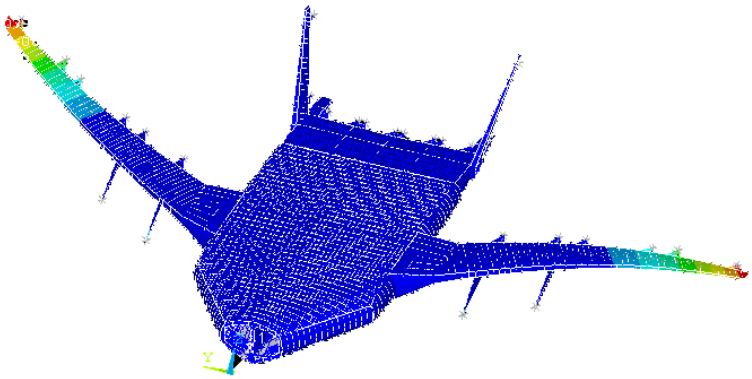

Figure 3.8: Shape of 2^{nd} mode.

The most significant modes of the aircraft are first symmetrical and anti-symmetrical wing bending modes (in frequency 1^{st} and 2^{nd} modes). Shape of the first and second aircraft mode modeled in ANSYS can be seen from Fig. 3.7 and 3.8. The target mode shapes of these modes are plotted in Fig. 3.9. For all next considerations we will assume these modes to be controlled and than we need to maximize information content of these modes in measurement.

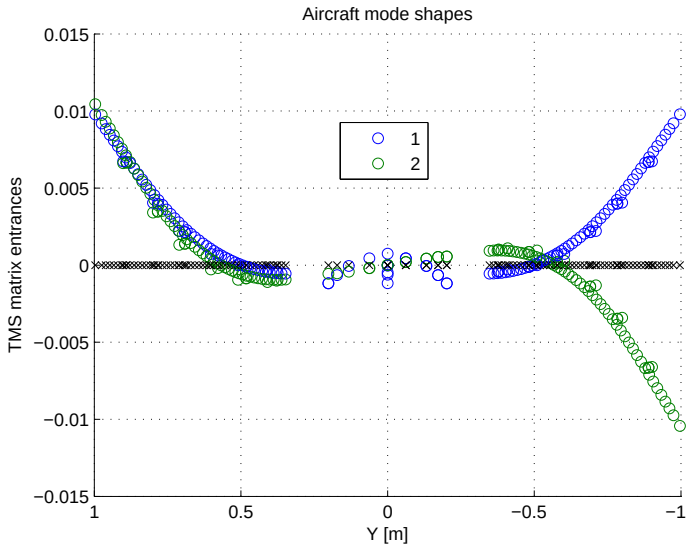

Figure 3.9: Shape of 1^{st} (blue o) and 2^{nd} (green o) modes and sensors reference positions with zero deflection (black x).

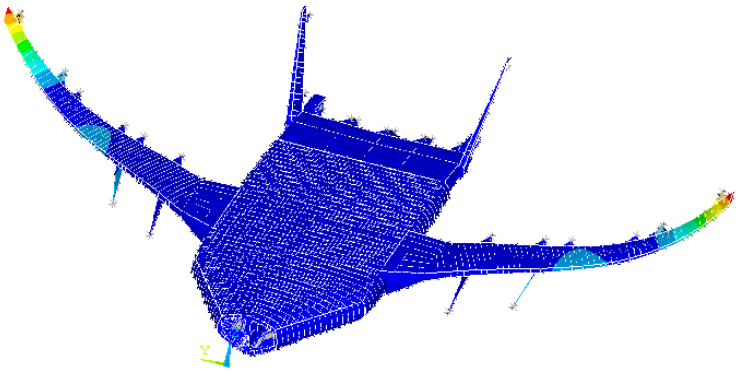

Figure 3.10: Shape of 3^{rd} mode.

The second symmetrical and anti-symmetrical modes, also called engine modes (in frequency 3^{rd} and 4^{th} modes) are considered as a non-controlled modes and we need to minimize information content of these modes in measurement. Shape of the third and fourth aircraft modes modeled in ANSYS can be seen from Fig. 3.10 and 3.11 and the target mode shapes are plotted in Fig. 3.12.

Results of optimization for case of first and second modes as required versus

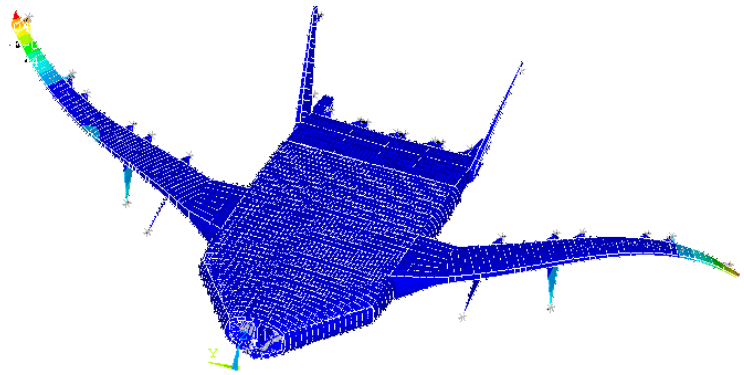

Figure 3.11: Shape of 4^{th} mode.

third and fourth modes to be rejected are plotted in Fig. 3.13. One can see that information content of required modes captured by this configuration of sensors is thousand times higher than information content of not-required modes (SNR approach 56dB).

Selected sensors are superimposed into target mode shapes. One can see from Fig. 3.14 that higher deflections of wings during first symmetrical and anti-symmetrical bending modes are at more outboard positions. On the other hand, the nodes (zero deflection of wings due to particular mode) of the second symmetrical and anti-symmetrical wing bending modes are situated in the second third of wings lengths as can be seen from Fig. 3.15. Sensors location optimization therefore results in positions near the most outboard nodes of the not-required modes.

The case of two highest modeled modes to be rejected is considered next. Last two modes in this case can be considered as a "high frequency noise" with defined spatial distribution to be filtered out by our OSP method. The 29^{th} and 30^{th} target mode shapes are plotted in Fig. 3.16.

Optimal sensors placement for the case of first symmetrical and anti-symmetrical modes versus last two symmetrical and anti-symmetrical modes is plotted in Fig. 3.17. Similarly as in the previous case, the most outboards sensors are involved due to nodes of not-required modes, but now also sensors in rear fuselage are selected. This behavior can be explained by comparison of target mode shapes

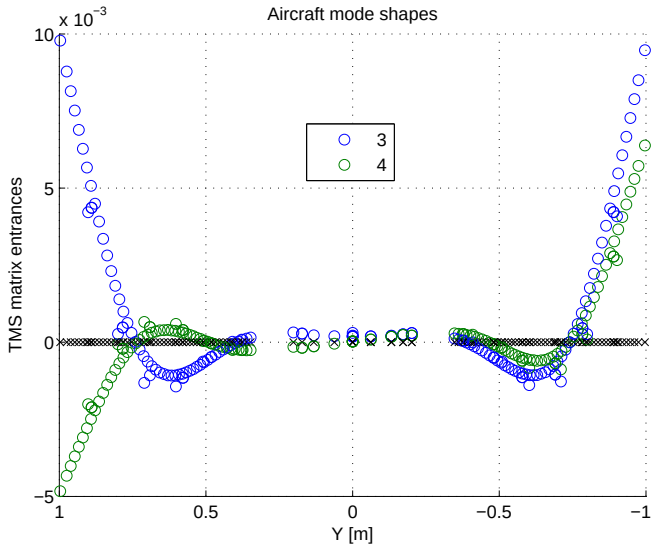

Figure 3.12: Shape of 3^{rd} and 4^{th} modes and sensors reference positions with zero deflection (black x).

plotted in Fig. 3.9 and Fig. 3.16. One can see a diving aircraft tail in case of first symmetrical wing bending mode and the fuselage rotation along longitudinal axis in the case of first anti-symmetrical wing bending mode (Fig. 3.9). On the other hand no deflection of fuselage occurs in 29^{th} and 30^{th} symmetrical and anti-symmetrical wing bending modes. This can also be seen from comparison of selected sensor sets superimposed into target mode shapes of required modes (Fig. 3.18) and undesirable modes (Fig. 3.19).

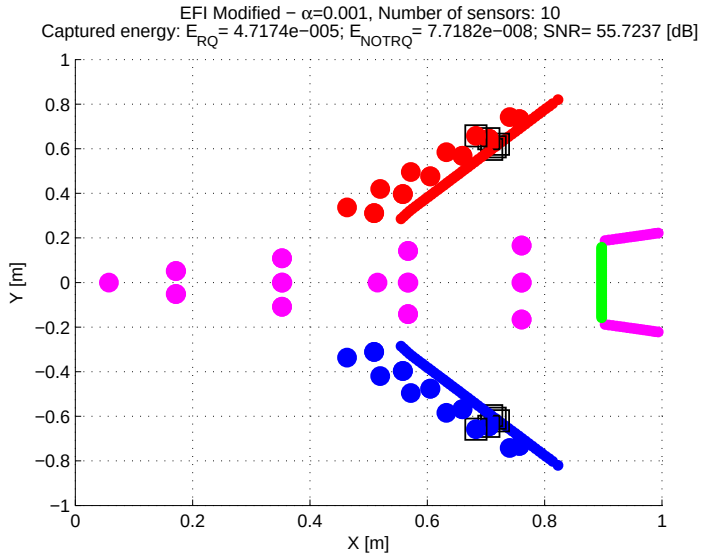

Figure 3.13: Optimal sensors positions.

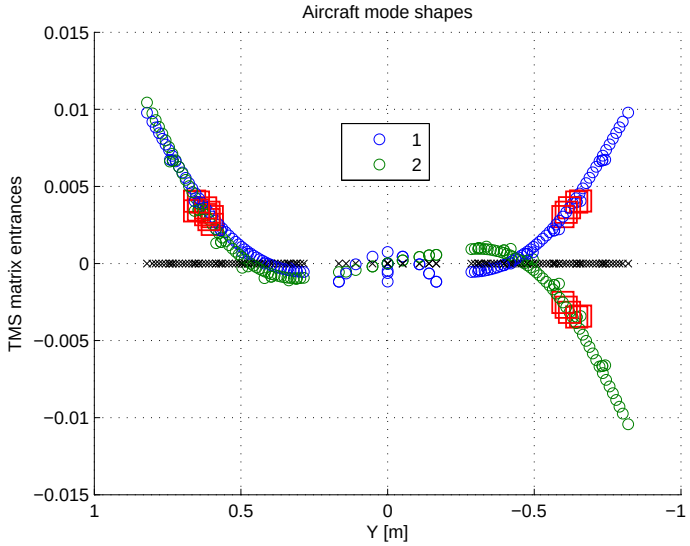

Figure 3.14: Optimal sensors positions (red squares) plotted in required modes shapes (1^{st} mode shape - blue o and 2^{nd} mode shape - green o) and sensors reference positions with zero deflection (black x).

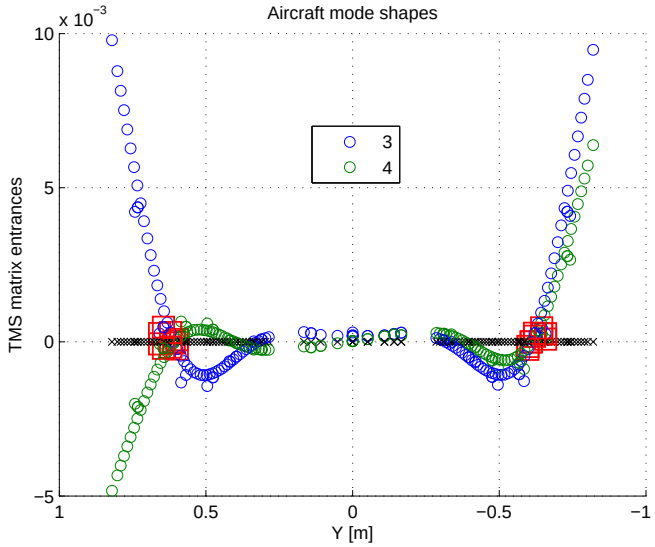

Figure 3.15: Optimal sensors positions (red squares) plotted in not-required modes shapes (3^{rd} mode shape - blue o and 4^{th} mode shape - green o) and sensors reference positions with zero deflection (black x).

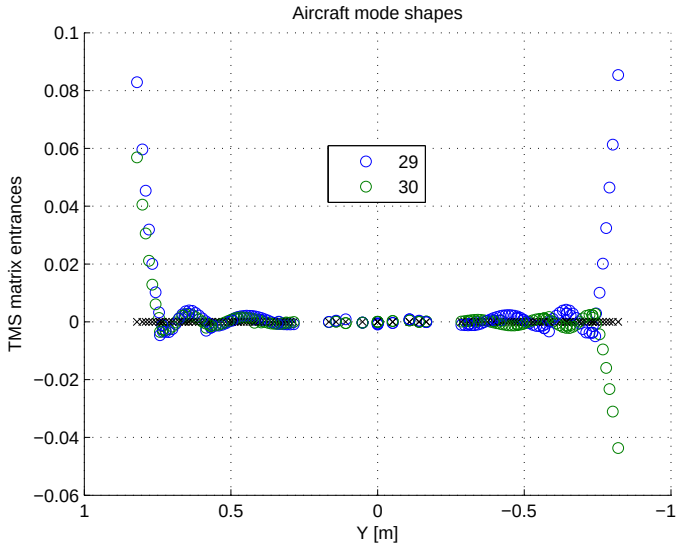

Figure 3.16: Shape of 29^{th} (blue o) and 30^{th} (green o) modes and sensors reference positions with zero deflection (black x).

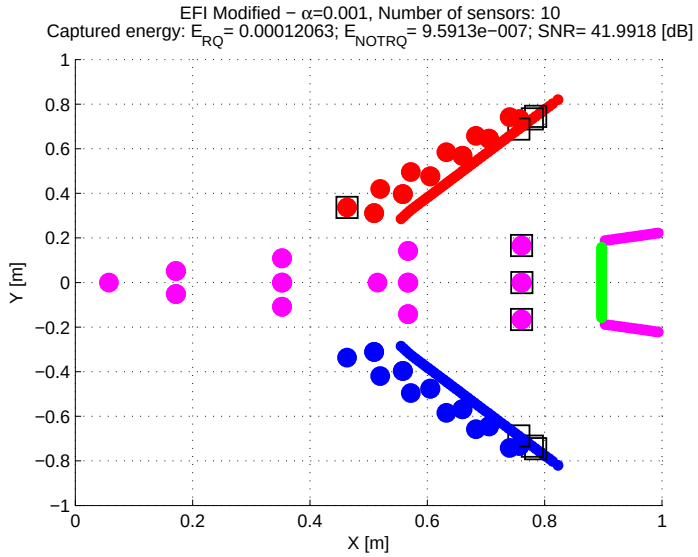

Figure 3.17: Optimal sensors positions.

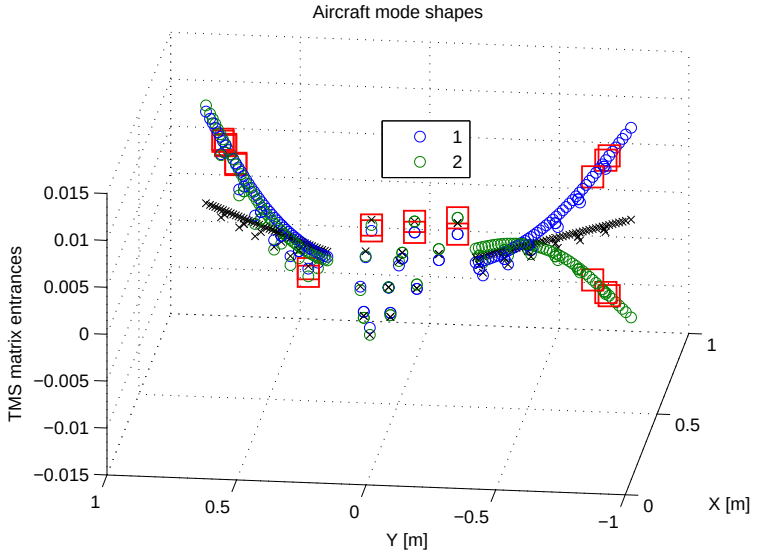

Figure 3.18: Optimal sensors positions (red squares) plotted in required modes shapes (1^{st} mode shape - blue o and 2^{nd} mode shape - green o) and sensors reference positions with zero deflection (black x).

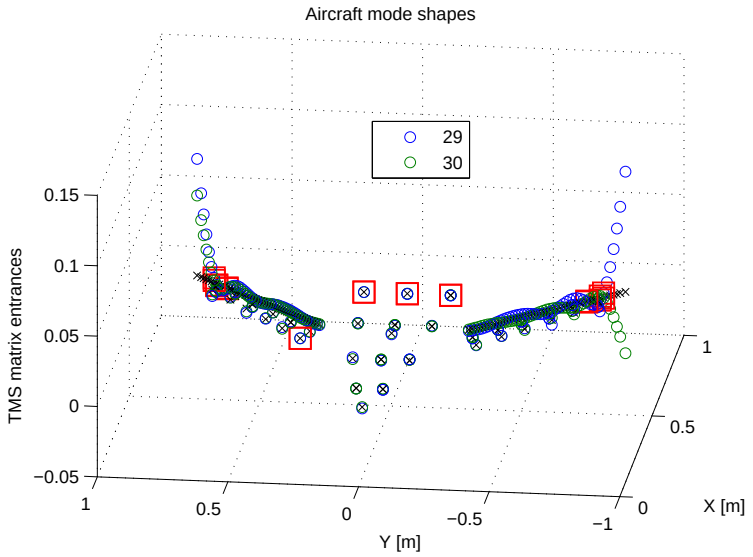

Figure 3.19: Optimal sensors positions (red squares) plotted in undesirable modes shapes (29^{th} mode shape - blue o and 30^{th} mode shape - green o) and sensors reference position with zero deflection (black x).

Chapter 4

H_∞ optimal feedback aircraft control

4.1 Lateral H_∞ optimal control law

Two different approaches for design of lateral control augmentation system for large blended-wing-body aircraft (BWB) with flexible structure are presented and asses in this section. The most challenging issue is handling of rigid-body dynamics and flexible modes coupling. First, a more classical approach is employed giving rise to separate flight dynamics controller (H2 optimal, with sufficient roll-off) and an active damper for most prominent lateral flexible modes on top of that (mixed-sensitivity H_∞ design). This approach proves successful and has obvious advantages related to the design process complexity, or implementation and testing issues. On the other hand, there is always a risk of potentially significant performance loss compared to a fully integrated design. For this reason, fully integrated design is also presented in the form of a fixed-order MIMO H_∞ optimal FCS controller, obtained by means of direct non-convex non-smooth optimization package HIFOO. Performance of both approaches is assessed.

4.1.1 Introduction

Large aircraft structures and novel concepts, such as Blended Wing Body (BWB) aircraft configurations, can lead to higher fuel-efficiency and reduced emissions. However, this also leads to low frequency structure vibration modes, and coupling of those to the flight mechanic modes may occur. Also, BWB concepts are expected to show coupling between longitudinal and lateral dynamics. This and significant parameter dependency of the aircraft dynamics pose significant design challenges for developing robust and well-performing flight control laws. Traditional methods for flight control design typically use nested SISO control loops and strongly structured control architectures (Stevens and Lewis, 2003). These methods are based on detailed aircraft system analysis and exploit paths with weak coupling to obtain good results for conventional flight control design. However, multivariate methods, such as optimal control and particularly robust control design methods are state of the art for more complex flight control tasks under coupled and/or uncertain system dynamics. Two large groups of control design methodologies are optimal control design methods (e.g., LQG control and the Kalman estimator (Lewis, 1986)), as well as robust control design methods (see (Zhou et al., 1996) and (Skogestad and Postlethwaite, 1996) for fundamentals, or (Bates and Postlethwaite, 2002) for an aerospace-specific overview). This work reports first findings from ongoing research connected to the control design for a large BWB passenger aircraft.

Two different approaches to lateral MIMO feedback Control Augmentation System (CAS) for NACRE BWB aircraft are presented in the following. They are namely a robust MIMO H_2/H_∞ mixed sensitivity controller and a low-order robust MIMO H_∞ optimal controller designed by direct fixed-order control design techniques. All controllers are designed to assure for desired closed-loop rigid-body response (namely rise time and no-overshoot behavior to the reference change of the bank angle set point, attenuation of beta disturbance, and required damping ratio of the DR mode) and to damp first two antisymmetric wings flexible modes. Performance and robustness of all controllers is demonstrated by means of MATLAB/Simulink simulations, and their advantages and drawbacks are discussed to arrive at conclusions. More details about BWB aircraft control issues

can by found in (Schirrer et al., 2010*a*), (Schirrer et al., 2010*b*), (Westermayer et al., 2010), (Westermayer et al., 2009).

4.1.2 Blended Wing Body aircraft lateral mathematical model

Mathematical model of BWB aircraft used for control law design consist of aircraft model itself, model of actuators and sensors. Actuators models are considered as 2^{nd} order linear models augmented by saturations and rate limiters. Sensors are modeled as 2^{nd} order Butterworth filters with time delays approximated by 2^{nd} order Padde approximation. Mathematical model of aircraft consist of rigid body description (modeled as a 12^{th} order linear system separated to longitudinal and lateral dynamics), flexible modes (for design purposes just four modes are considered, with rise to 8^{th} order linear model) and lag states. Overall model used for control law design is of order 52.

4.1.3 H2/H_∞ mixed sensitivity controller

A two-stage control law is devised - separate control augmentation system (CAS) taking care of the flight-dynamics (robust H_2 optimal roll autopilot, with roll-off at higher frequencies), and an active damper for selected flexible modes (H_∞ optimal mixed-sensitivity controller tuned to first two antisymmetric wing bending modes). Such an arrangement has obvious advantages - regarding tuning (both parts are designed/tuned independently), future flight testing (the active damper can be tested after the roll autopilot is implemented and approved, and it can be turned on/off at any time while keeping the aircraft well controlled), safety (loss of the damper's functionality, e.g. due to sensors failure, does not take the airplane out of control). The drawback is potential reduction of performance compared to a fully integrated design where both flight dynamics and vibrational issues are handled by a single large multiple input multiple output (MIMO) controller.

4.1.3.1 Design method

The lateral CAS (roll autopilot) is designed by H_2 norm minimization of the generalized plant, encompassing the lateral rigid body dynamics itself (4 states/outputs), 2 integrators (to assure for perfect steady-state tracking of roll angle set point

command and for perfect steady-state attenuation of beta disturbance), and two low-pass filters (for required roll-off at higher frequencies - so that the flexible modes are left untouched, not excited by the controller). As all the rigid body (RB) states are measured, the observer needs not be implemented in fact and the resulting order of this CAS can be kept quite small (six states). Resulting controller features robust stability/performance for all considered mass cases (3 passengers and 5 fuel cases).

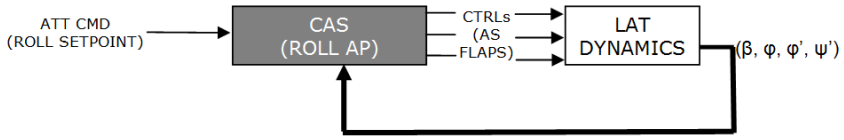

Figure 4.1: Control augmentation system for H_2 controller design. Where control surfaces are considered as anti-symmetrically driven wings ailerons.

On top of that, a robust MIMO controller is built by minimization of the H_∞ norm of the frequency weighted mixed-sensitivity function. Wings modal antisymmetric sensor and antisymmetric flaps make up the input/output groups. Loosely speaking, the closed loop sensitivity function is kept small at selected frequency regions (in our case covering the wing antisymmetric modes) to assure for good performance (disturbance attenuation) while the complementary sensitivity function is kept small everywhere else (to assure for robustness - the design model becomes invalid outside the selected frequency region). A simple design model of 8th order was constructed (modeling accurately the two modes and close region in the I/O channels). Two resonant weighting filters of 2^{nd} order are tuned to the frequencies and dampings of the antisymmetric wing bending modes of a selected representative case for this purpose. Resulting H_∞ controller has 20 states.

Resulting damper (and also the overall CAS/damper combo) features robust stability for all mass cases, significant improvement regarding damping of structural vibrations for major part of mass cases (more than 5dB attenuation), and no-effect on vibrations damping for the remaining cases. These findings, and the overall performance of the designed controller and its respective parts, are visualized in the Fig. 4.1 and Fig. 4.2.

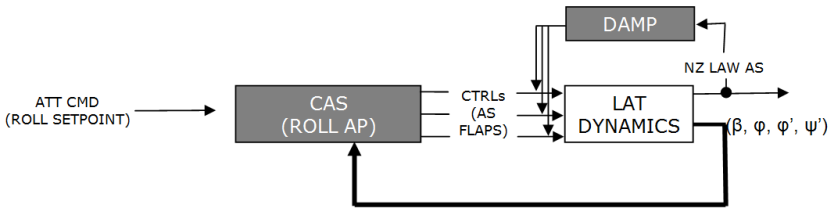

Figure 4.2: Control augmentation system for H_2/H_∞ controller design. Where control surfaces are considered as anti-symmetrically driven wings ailerons.

4.1.3.2 H2/H_∞ control results

Brief assessment of the controller performance is given in the text above (regarding robustness and performance). A set of selected characteristics is now given to document those findings.

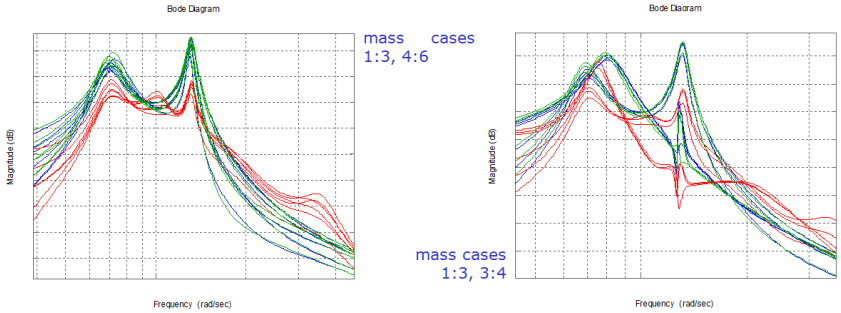

Figure 4.3: Wing bending mode. Open loop (green), H_2 control (blue) and H_2/H_∞ control (red). All axis values are omitted from confidential reasons.

Note that very good performance is achieved for those cases that do not vary much in the frequency of the targeted modes (Fig. 4.3 left). However, even for the other cases (Fig. 4.3 right), some performance improvement is achieved, and robust closed loop stability is assured.

Required response to a set point command is achieved. Note marginal improvement of the response when the damping system is connected (though it was not intended to influence the flight dynamics in fact). As stated above, the flight-dynamics part contains integrated yaw damper and beta compensator. Gain and

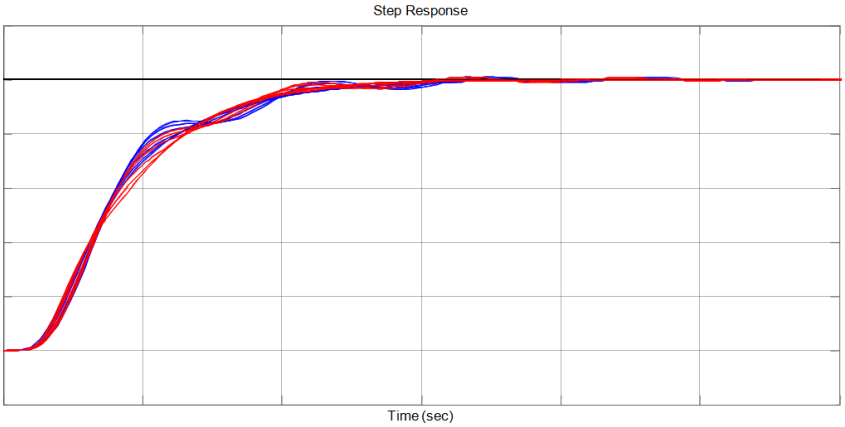

Figure 4.4: Roll reference tracking. H2 control (blue) and H_2/H_∞ control (red).

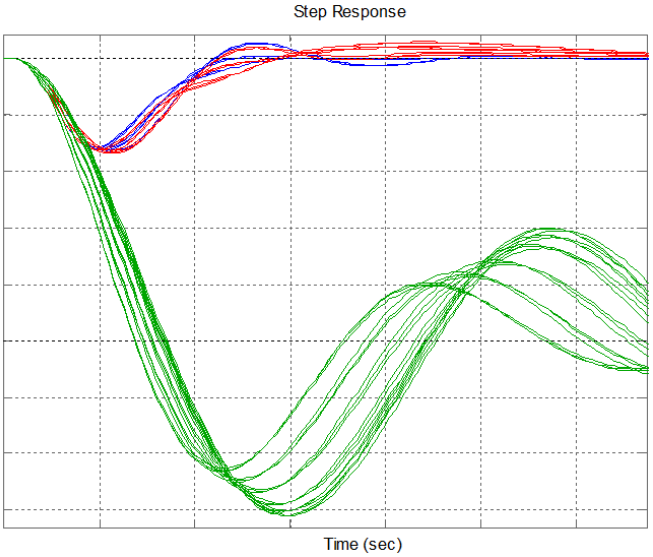

Figure 4.5: Beta disturbance rejection. Open loop (green), H_2 control (blue) and H_2/H_∞ control (red).

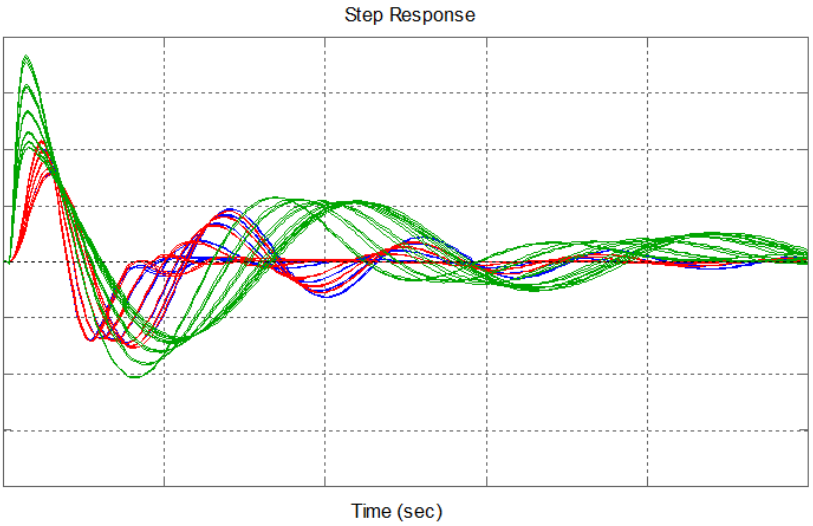

Figure 4.6: Yaw rate damper. Open loop (green), H_2 control (blue) and H_2/H_∞ control (red).

phase margins for the complete designed controller have been evaluated. Robust closed loop stability for all mass cases is achieved. For simultaneous, independent, worst-case variations in the individual channels the gain margin ranges $\pm 1.9 - 3.7dB$, phase margin $\pm 12 - 23$ degrees, depending on the mass case (MATLAB/Robust Control Toolbox command *loopmargin*).

4.2 Non-convex non-smooth optimization

In recent years, a great progress has been made in the challenging area of non-convex non-smooth optimization solvers. In contrast to more traditional setups, such problems are highly non convex and no differentials or Jacobians can be used to navigate the search for even a local optimum. The solvers rely on BFGS (Broyden-Fletcher-Goldfarb-Shanno) variable metric (quasi-Newton) method (Lewis and Overton, 2009), (Burke et al., 2005), (Burke, Lewis and Overton, 2006), or nonsmooth modification of Virginia Torczon's multidirectional search (MDS) (Torczon, 1991), (Torczon, 1997), (Apkarian and Noll, 2006).

Related numerical software has been soon delivered in the form of freeware

and commercial package like Hybrid Algorithm for Non-Smooth Optimization (HANSO) based on BFGS method.

As people from the systems and control community quickly realized, such algorithms and tools can be successfully applied to resolve some control design problems that are otherwise almost untractable for real-life problems. Didier Henrion and Mike Overton seem to get furthest, proposing a new methodology for direct design of low-order H_∞ optimal controllers in 200x, (Gumussoy et al., 2009), (Arzelier et al., 2011), (Gumussoy et al., 2008), (Gumussoy and Overton, 2008), (Millstone, 2006), (Burke, Henrion, Lewis and Overton, 2006), and delivering a related freeware package HiFOO.

The HiFOO package has already attracted attention of controls designers in the miscellaneous field (Robu et al., 2010), (Pouly et al., 2010), (Delwiche, 2009), (Dotta et al., 2009), (Wang and Chen, 2009), (Knittel et al., 2007). Regarding flight controls design, the first attempt was made in master thesis (Millstone, 2006), where the applicability of the package was approved by a means of a textbook-example of wing-leveller controller for an F-16 aircraft.

In this thesis, this approach and software will be employed to design, at one-shot, a robust, full-featured, H_∞ optimal longitudinal control law for a BWB highly flexible near-future airliner concept, following the recommended and industry-approved structure for this CAS system. Performance of the result is assessed by means of high-fidelity simulations and classical, industry-standard robustness analysis results.

4.3 Direct approach to fixed-order H_∞ optimal control design

For reader's reference, the basic principles of the underlying algorithms used for direct H_∞ fixed-order control design are summarized in brief in this section, adopted from (Gumussoy et al., 2009). Interested readers are advised to consult the original papers for a more detailed and rigorous treatment.

The aim of HiFOO algorithm is to deliver stabilizing H_∞ optimal controller for given n LTI systems. Where the criterion for H_∞ optimization is expressed by

generalized plant set up. The algorithm has two phases. In each phase the main workhorse is the BFGS optimization algorithm, which is surprisingly effective for nonconvex, nonsmooth optimization. The user can provide an initial guess for the desired controller; if this is not provided, HiFOO generates randomly generated initial controllers, and even when an initial guess is provided, HiFOO generates some additional randomly generated initial controllers in case they provide better results. The first phase is stabilization: BFGS is used to minimize the maximum of the spectral abscissa of the closed loop plants. This process terminates as soon as a controller is found that stabilizes these plants, thus providing a starting point for which the objective function for the second phase is finite. The second phase is optimization: BFGS is used to look for a local minimizer of the controllers found at firs phase. The HiFOO control design method searches for locally optimal solutions of a non-smooth optimization problem that is built to incorporate minimization objectives and constraints for multiple plants. Where the optimization problem is introduced as a set of augmented plants, see Figure 4.7, commonly used in robust control approaches. First, the controller order is fixed at the outset, allowing for low-order controller design. Second, no Lyapunov or lifting variables are introduced to deal with the conflicting specifications. The resulting optimization problem is formulated on the controller coefficients only, resulting in a typically small-dimensional non-smooth non-convex optimization problem that does not require the solution of large convex sub-problems, relieving the computational burden typical for Lyapunov LMI techniques. Simultaneously proved you with capability to fix some entries in controller Rosenbrock matrix, in this particular case it is possible to prescribe zero entries. Because finding the global minimum of this optimization problem may be hard, an algorithm that searches only for local minimization is used. While no guarantee can be given on the result quality of this algorithm, in practice it is often possible to determine a satisfying controller efficiently.

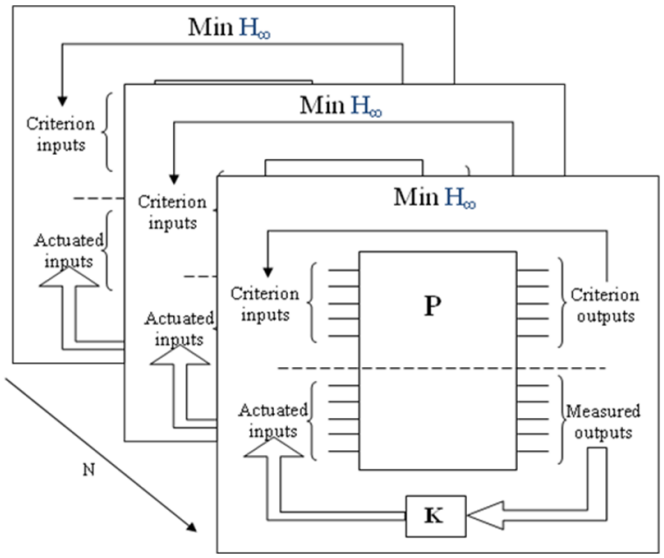

Figure 4.7: H_∞ fixed order optimization setup.

4.3.1 Lateral fixed order H_∞ optimal MIMO robust controller

An integrated H_∞ optimal approach was used to design Lateral Control Augmentation System (CAS) for BWB airliner. Similarly as in previous section two different control goals were aimed, but this time in one integrated version. One part of control law is to provide autopilot functionality. The autopilot consists of Stability Augmentation System (Dutch roll damper) and CAS (roll and beta angle reference signal tracking). Other part of control law takes care of vibration and load attenuation.

The lateral integrated CAS was designed as a 2DoF architecture using fixed order optimization approach to keep control law order low. The resulting extremely low order (in this case 3^{rd} order control law was used) controller was built using HiFOO toolbox. Overall lateral CAS consist of Rigid Body autopilot (roll and beta tracker with Dutch roll damper) and structural modes control. The lateral CAS set up can be seen from Fig. 4.8. Two reference signals are used as inputs into feedforward part of controller (roll and beta set points). The beta reference signal is usually set to zero and then CAS provides coordinated turn functionality.

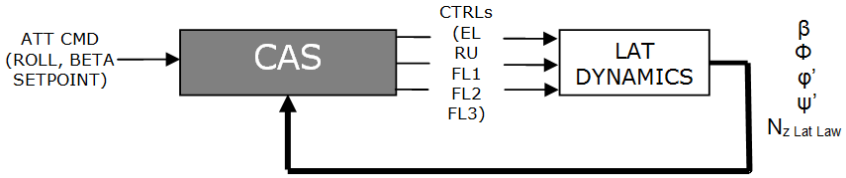

Figure 4.8: Control augmentation system for HiFOO.

Control surfaces used by CAS are all ailerons (antisymmetricaly actuated FL1 - FL3), rudders (RU) and elevators (symmetrically actuated EL). Measured signals are lateral RB variables at CG (beta angle, roll angle, roll rate and yaw rate), for structural modes control we have selected lateral wing acceleration modal sensor in antisymmetrical setup. Resulting control law (autopilot and structural modes controller) provides robust stability as well as robust performance for all 18 cruse conditions cases (6 fuel and 3 passenger cases).

4.3.1.1 HiFoo control results

Improvement of damping of 1^{st} and 2^{nd} wing bending modes can be seen form Fig. 4.9. Simultaneously DC gain is preserve for all cases. Robust performance property can be seen form Bank angle reference signal tracking response plotted in Fig. 4.10 (left). Response for series of two steps is involved here and one can see that handling qualities are satisfied with suitable amount of overshot.

Property of beta disturbance attenuation is investigated in Fig. 4.11 (left). One can seen complete vanishing of side wing influence in few second and without inducing of oscillation for major part of cases. Dutch roll mode damping is investigate in Fig. 4.11 (right).

Gain and phase margins for the complete designed controller have been evaluated. Robust closed loop stability for all mass cases is achieved. For simultaneous, independent, worst-case variations in the individual channels the gain margin ranges $\pm 0.8 - 2.6dB$, phase margin $\pm 5 - 16$ degrees, depending on the mass case (MATLAB/Robust Control Toolbox command *loopmargin*).

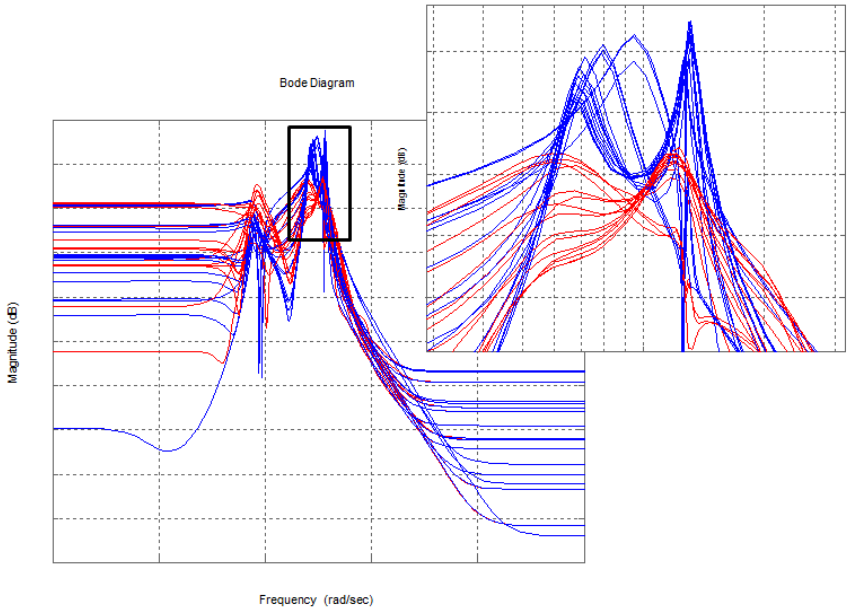

Figure 4.9: Wing bending mode. Open loop (blue), closed loop (red).

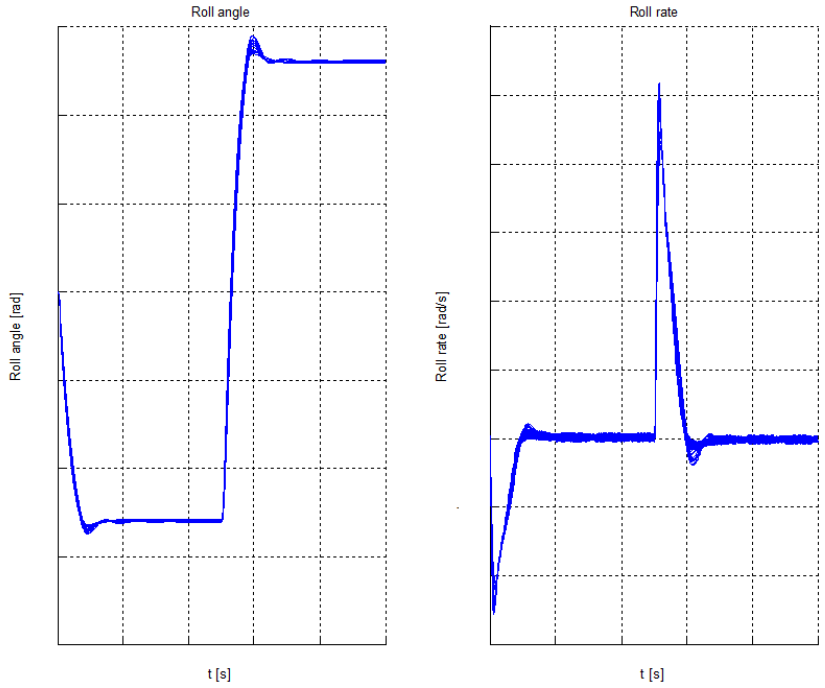

Figure 4.10: Bank angle and Roll rate reference signal tracking.

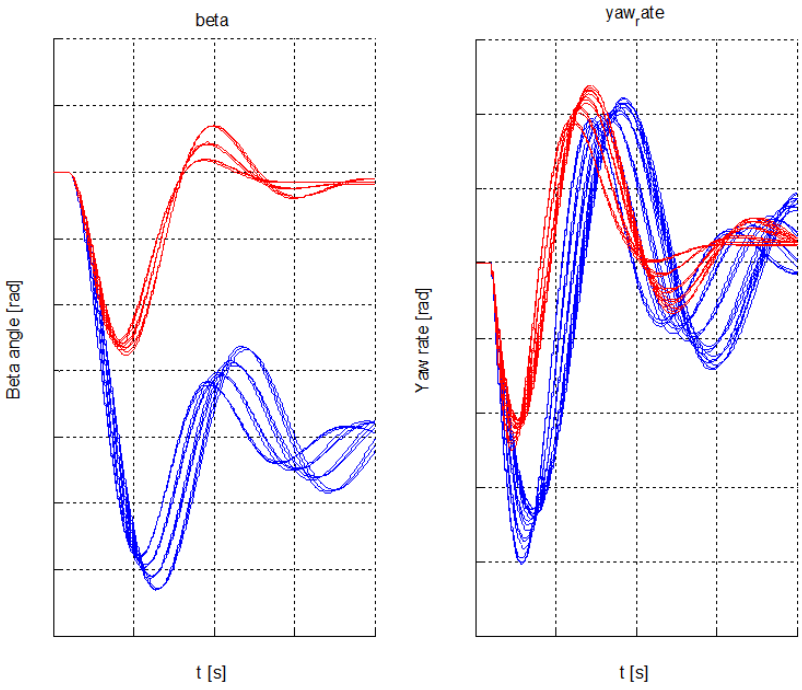

Figure 4.11: Beta angle disturbance attenuation (left) and Yaw rate damping (right). Open loop (blue), closed loop (red)

4.4 Longitudinal H_∞ optimal control law of prescribed structure

Advanced non-convex non-smooth optimization techniques for fixed-order H infinity robust control are proposed in this part for design of flight control systems (FCS) with prescribed structure. Compared to classical techniques - tuning of and successive closures of particular single-input single-output (SISO) loops like dampers, attitude stabilizers etc. - all loops are designed simultaneously by means of quite intuitive weighting filters selection. In contrast to standard optimization techniques, though (H_2, H_∞ optimization), the resulting controller respects the prescribed structure in terms of engaged channels and orders (e.g. P, PI, PID controllers). In addition, robustness w.r.t. multi model uncertainty is also addressed which is of most importance for aerospace applications as well. Such a way, robust controllers for various Mach numbers, altitudes, or mass cases can be obtained directly, based only on particular mathematical models for respective combinations of the flight parameters.

4.4.1 Introduction

The flight dynamics, exhibiting many oscilatory or unstable modes for a typical aircraft, as well as the automatic or semi-automatic regimes of modern autopilots call for control synthesis methods that can effectively address these issues. Traditionally, classical tools for SISO loops tuning are used successively to deliver a complex FCS composed of a few smartly pre-selected channels, like pitch, roll or yaw dampers for suitable dynamics modifications (stability augmentation), subsequent attitude hold autopilots, automatic navigation loops, etc. Typically, a significant number of iterations and "backstepping" is required as the higher-level loops interact partially with the lower-level pre-designed parts. Historically, frequency response methods were developed first in the 1930's and 1940's (Miller, 1966), (McRuer et al., 1973), (Evans, 1948), (Blakelock, 1965), (Perkins, 1970), and they remain arguably the most commonly used methods till these days (Bryson, 1994).

Since the 1960's, results of the optimal control theory have been used extensively for the aircraft controls design as a powerful alternative to the classical

approach. The methods are typically purely MIMO (multiple-input multiple-output) by their nature, delivering all channels of the resulting controller at "one shot". The design procedure is controlled indirectly by means of selection of some weightings, being it constant matrices for LQ or LQG approach (Lewis and Syrmos, 1995), (Zhou et al., 1996), or LTI (linear time invariant) shaping filters for the H_2 or H_∞ optimal control (Zhou et al., 1996), (Skogestad and Postlethwaite, 1996), (Bates and Postlethwaite, 2002). Nevertheless, the structure of the FCS is typically very hard or impossible to imprint, and the order (complexity) of the resulting controller can become unexceptably large as well. In this regard, the classical methods still have quite a lot to offer.

Robustness of the flight controller is of utmost importance. The dynamics of flight changes considerably as the aircraft properties vary over time (fuel amount, center of gravity position) and as the flight parameters change (altitude, airspeed, attitude angles). Classical and optimal controllers must fulfill the robustness requirements which is typically acknowledged by means of stability margins analysis (gain margin, phase margin, p. 181 in (Lewis and Syrmos, 1995), p. 237 in (Zhou et al., 1996) or p. 31 in (Skogestad and Postlethwaite, 1996) and (Chopra and Ballardf, 1981), (Chang and Hant, 1990), (Perng, 2004)) and extensive simulations for selected important points of the flight envelope. Nevertheless, neither of these methodologies is intended to incorporate the robustness requirements explicitly into the design procedure. In contrast, the robust control design approach, developed in the 1980's through 2000's, (Zhou et al., 1996), (Doyle, 1979), (Doyle, 1982), (Doyle et al., 1989) relies on the mathematical formulation of the uncertainty as one of the control design parameters. Most prominent methods are unstructured H_∞ optimization (Zhou et al., 1996), (Skogestad and Postlethwaite, 1996), (Bates and Postlethwaite, 2002), structured H_∞ control (mu synthesis, DK iterations, (Zhou et al., 1996), (Doyle et al., 1982), (Doyle and Packard, 1987), (Balas et al., 1991), (Doyle et al., 1987), robust loopshaping (McFarlane et al., 1992), and others. They all have been naturally accepted by the aerospace controls community, giving rise to significant implementations (Bennami and Looye, 1998), (Fialho et al., 1997), (Hyde, 1995), (Postlethwaite et al., 1999).

One may ask if there is not a way to combine the benefits of the classical, optimal and robust approaches - the convenient weighting-filters formulation of the

optimal control synthesis, hierarchical and comprehensive structure of the classical controllers, and insensitivity to parameters uncertainties of the robust control designs. And there has been some attempts made indeed, based either on linear quadratic optimization (static output feedback design (Stevens and Lewis, 2003), (Stevens et al., 1983), (Stevens et al., 1992)), or based on mixed-sensitivity H_∞ optimization with static output constrains (Kureemun and Bates, 2001), (Skelton et al., 2007), or mixed H_2/H_∞ optimal controller of fixed order based on homotropy algorithm (Whorton et al., 1996).

In this paper, a completely different approach towards this goal is suggested though. Thanks to practical availability of CACSD tools (Computer Aided Control Systems Design tools) based on most recent non-convex non-smooth optimization techniques, direct synthesis methods can be employed to deliver a complex FCS that is structured (features pre-selected channels only), of fixed low order (consisting of e.g. P, PI, lead-lag controllers), optimal in the H_∞ norm sense (for bandwidth setting, reference tracking, disturbance attenuation requirements), and robust w.r.t. multi model uncertainty (covering a selected number of airspeed, mass, altitude, or other cases).

The rest of this section is structured as follows. In section 4.3 the non-convex non-smooth optimization techniques for fixed order controller design are reviewed in brief. Related CACSD tools are introduced in section 4.4.2. The main result of the paper is the case study presented in section 4.4.2 (where new methodology for longitudinal CAS system is presented) and in section 4.4.3 (where advanced case study is presented). The procedure towards a structured, low complexity, and robust lateral FCS is elaborated in detail for a nonlinear model of a BWB type aircraft, as a proof of practical usefulness of the proposed modern techniques for flight controls design purposes.

4.4.2 Longitudinal structured control law with HIFOO

We propose a systematic methodology for one-shot, robust, full-featured, H_∞ optimal longitudinal control design, for a multi-model case covering substantial points of the flight envelope. This methodology literally combine advantages from modern controller design techniques involving H_∞ or H_2 optimization with hierarchical

approach for aircraft control system design. HiFOO toolbox preserve property of physical meaning of each control system loop (which is reasonable argument of aircraft control system engineers) and remove disadvantage of loop by loop tuning of control systems. On the other hand the techniques as generalized plant set up as well as criterion definition in frequency domain (weightings filters like used in (Schirrer et al., 2010*a*), (Schirrer et al., 2010*b*), (Westermayer et al., 2010), (Westermayer et al., 2009)) are involved to delivery multi input multi output controller, well known from H_∞ optimization. Still HiFOO toolbox can be understand as a extension to the classical control design techniques. Due to local optimization property it is really time saving to provide HiFOO toolbox with suitable starting point. The standard hierarchical approaches can be than used as a most promising initial control law.

Algorithm:

Given:

- Set of systems for control design
- Structure of resulting control law
- Criterion.

Output:

- Robust LTI control law with predefined structure.
- **Step 1:** Specify generalized plant set up (define measurable outputs/actuated inputs and criterion by performance inputs/outputs).
  - **Recommendations:** It is needed to select measurable outputs/actuated inputs in correspondence to structure you want to design.
- **Step 2:** Specify performance requirements by weighting filters.
  - **Recommendations:** Depends on control problem. Typically low pass filters are used for reference signal tracking, or band pass filters are used for vibration modes attenuation.
- **Step 3:** Specify the control law structure.

  - **Recommendations:** The structure needs to be defined by controller Rosenbrock matrix. There can be more than one representation, try to fit minimal realization.

- **Step 4:** Specify the starting control law if any is available, otherwise it will be generated randomly.

  - **Recommendations:** The suitable choice of starting point is critical for time saving. The control law designed by classical approach can be the most suitable choice.

- **Step 5:** Run HiFOO toolbox.

  - **Recommendations:** The involved optimization does not guarantee global optimum, therefore it is usually required to run optimization several times to avoid sticking in local optimum.

The longitudinal Control Augmentation System (CAS) of extremely low order (1st order control law) with imprint structure was design by HiFOO toolbox. The structure of control law is shown in Figure 4.12, respectively Figure 4.13 (with mapping of constants (4.1)).

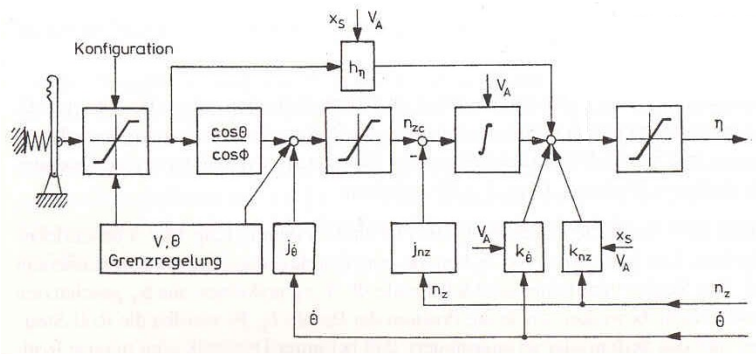

Figure 4.12: Longitudinal Control Augmentation System.

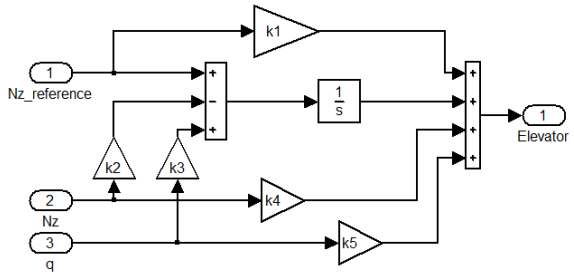

Figure 4.13: Normal acceleration reference signal tracking Control Augmentation System with structure.

$$\begin{aligned} k_1 &= h_\eta \\ k_2 &= j_{nz} \\ k_3 &= j_{\dot{\theta}} \\ k_4 &= k_{nz} \\ k_5 &= k_{\dot{\theta}} \end{aligned} \tag{4.1}$$

It is a common hierarchical control law used for an asymptotic tracking of the aircraft normal acceleration reference signal (see (Brockhaus, 2001), (Stevens and Lewis, 2003)). The hierarchical control law design was usually done in the iterative manner, using background knowledge of the physical meaning of the single loop to reach required performance. The optimization technique is addressed now to design the overall control law in one shot. H_∞ performance criteria can be introduced to design robust control law with predefined structure and order. The extremely low order and structural complexity of overall control law (with preserved robust behavior and control performance of full MIMO high order control laws) is very important for final on-board implementation. It reduces necessary computational effort and therefore hardware demands for on-board equipment, which is closely connected with reliability and price of implementation. For other possibilities of high order MIMO CAS designs see (Schirrer et al., 2010*a*), (Schirrer et al., 2010*b*), (Westermayer et al., 2010), (Westermayer et al., 2009). Control surfaces used by CAS are symmetrically actuated beaver tails (denoted as BT) and elevator (denoted as EL), in our case both flaps are actuated as one. Measured signals are longitudinal RB variables at CG, namely normal acceleration (denoted as Nz_{CG}) and pitch rate (q). Highly valuable feature of H_∞ optimization is

possibility to introduce robust behavior. The HiFOO toolbox will be used, in this particular case, to cover multiple plants each representing different fueling point of flight envelope to end up with longitudinal CAS robust with respect to fueling. Augmentation plant used for control law design is shown in Figure 4.14.

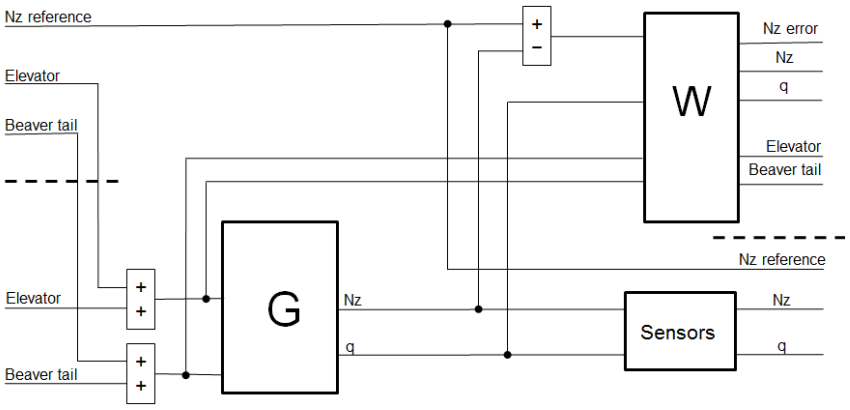

Figure 4.14: Augmentation plant set up used for longitudinal control law design.

Signal in the augmentation plant are divided into exogenous inputs and outputs (which represents control law performance by definition of optimization criterion), measured outputs and actuated inputs, according to Figure 4.7. Plant G represent aircraft longitudinal dynamic itself and weighting filters W represents definition of performance criterion in frequency domain. We are ready to introduce structure into HiFOO, by prescribing of zero entries in to controller Rosenbrock matrix, now. Let state space representation of controller is $K.a$, $K.b$, $K.c$ and $K.d$ than Rosenbrock matrix is:

$$K = \begin{bmatrix} K.a & K.b \\ K.c & K.d \end{bmatrix}, \tag{4.2}$$

with augmentation plant set up shown in Figure 4.14 and desired structure of controller shown in Figures 4.12 and 4.13 we can write controller in form:

$$A_K = 0 \tag{4.3}$$

$$B_K = \begin{bmatrix} 1 & -k_2 & k_3 \end{bmatrix} \tag{4.4}$$

$$C_K = \begin{bmatrix} 1 \end{bmatrix} \tag{4.5}$$

$$D_K = \begin{bmatrix} k_1 & k_4 & k_5 \end{bmatrix}. \tag{4.6}$$

We can wright controller Rosenbrock matrix now, in a form:

$$K = \begin{bmatrix} 0 & 1 & -k_2 & k_3 \\ 1 & k_1 & k_4 & k_5 \end{bmatrix}. \tag{4.7}$$

HiFOO toolbox can be applied now to process fixed order optimization with predefined structure of controller. When the controller is received. Final control law is integrated first order Multiple Input Single Output (MISO) controller with predefined structure and can be used as a integrated longitudinal CAS. However because of structure it is possible to disassembling for hierarchical structure of SISO loops, which can be used one by one as a Stability Augmentation System (SAS) itself (pitch rate damper and normal acceleration damper) as it is known from text books and longitudinal Control Augmentation System (CAS) in this case normal acceleration reference signal tracker.

4.4.3 BWB case study

4.4.3.1 Mathematical model of an aircraft longitudinal dynamic

Longitudinal flight mechanics and aero-elastic effects of a large blended wing body aircraft design and their coupling were modeled in and integrated. In this section, the longitudinal dynamics is considered to design control law for the longitudinal motion. A set of linearized state space systems for various parameter values of fuel and payload mass (at fixed cruise altitude and airspeed) are available:

$$\begin{aligned} \dot{x} &= A \cdot x + B \cdot u \\ y &= C \cdot x + D \cdot u \end{aligned} \tag{4.8}$$

where the state vector x is composed of the 6 flight-mechanic states (x-position X, body forward speed u, altitude Z, body down speed w (it is proportional to

angle of attack α), pitch angle θ and pitch rate q), 12 elastic states (6 symmetrical structural modes), as well as 7 aerodynamic lag states. The states X (x-position) and Z (altitude) are neglected in this study. Utilized inputs u for control design are:

- Symmetric Extended Elevator deflection δ_{EEL} $[rad]$ and deflection rate $\dot{\delta}_{EEL}$ $[rad/s]$.
- Symmetric Elevator deflection δ_{EL} $[rad]$ and deflection rate $\dot{\delta}_{EL}$ $[rad/s]$.

The Extended Elevator and Elevator control surfaces are coupled and actuated simultaneously (will be notated as δ_{EL}) in case of longitudinal control law. The actuator dynamics are modeled via 2^{nd} order low-pass filters.

Utilized outputs for control design are:

- Pitch rate q $[rad/s]$
- Normal acceleration Nz_{CG} $[m/s^2]$

where in both sensor signals 160ms time delay (due to signal processing latency, modeled via a 2^{nd} order Pade approximation) and low-pass Butterworth filters of 2^{nd} order were considered.

4.4.3.2 Simulations

The resulting longitudinal control law performance is presented in this section. First are presented linear model simulation in Matlab and than nonlinear Matlab Simulink model is involved to demonstrate longitudinal control law capabilities. Position of the closed loop poles is constrained by required relative damping of 0.5 for all rigid body poles, the only exception is for the phugoid mode, which can have even one real unstable pole with time period less than 0.1. The closed loop poles locations can be seen inFigure 4.15.

The aircraft normal acceleration step response can be seen in Figure 4.16, where the design plant (without phugoid mode) response as well as the validation plant (with phugoid mode) responses are plotted for all fuel cases (which is one of the robust behavior requirements).

The robustness of control law with respect to unmodelled uncertainty is presented. The uncertainty is here illustrated by diamonds in a Nichols charts, as

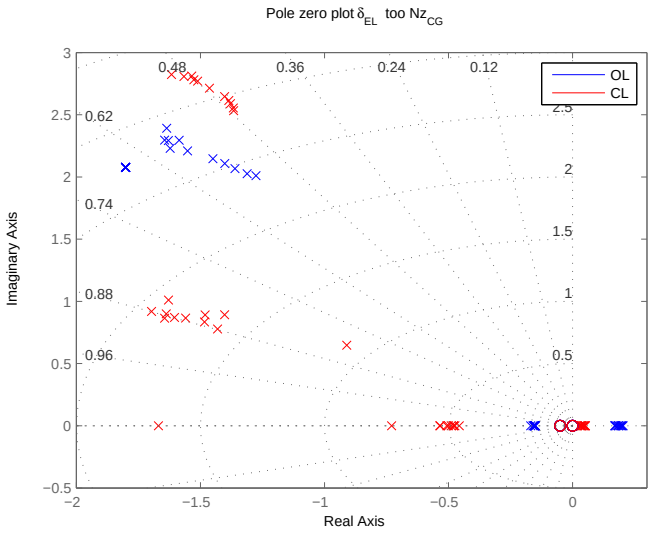

Figure 4.15: Poles and zeros plot of Nz_{CG} reference signal into Nz_{CG} output signal (ten fueling cases are plotted).

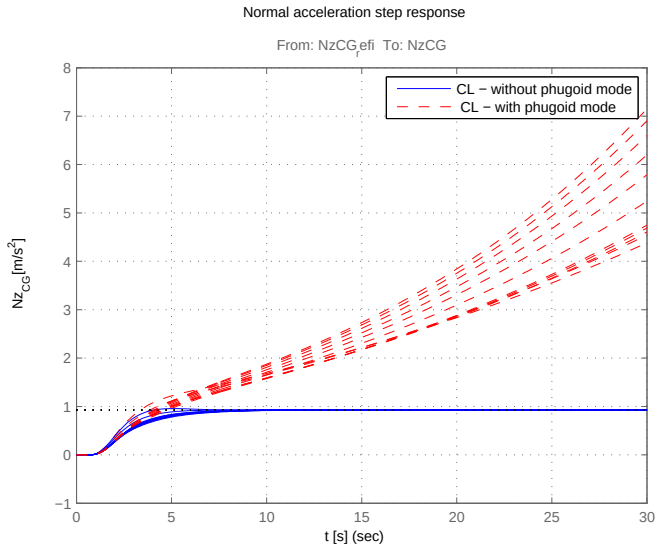

Figure 4.16: Normal acceleration step response - Matlab linear model simulation (ten fueling cases are plotted).

standard margins or robustness evaluation measures among aircraft controls designers for decades. Uncertainty in this case should by understand as a phase lag and gain variance insensitiveness. One Nichols chart is used for each opened loop (closed loop is disconnected at controller inputs or its output) of multiple inputs and single output control law to validate controller robustness. There are different robustness requirements for predefined frequency regions of control law, bounded by phugoid mode frequency (solid line diamond), short period frequency (dot and dash line diamond) and the first wing bending mode frequency (doted line diamond). First is investigated the robustness with respect to unmodeled uncertainty at system input, represented by diamonds in a Nichols chart of open loop transfer function from system δ_{EL} input to controller δ_{EL} output, see Figure 4.17 and its zoom in Figure 4.18. One can see that all curves are outside of prescribed diamonds which guarantee required robustness.

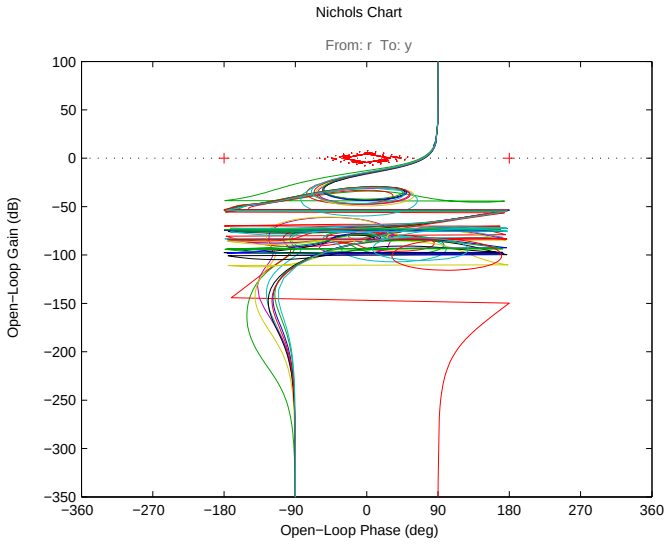

Figure 4.17: Nichols charts of closed loop disconnected at actuators (ten fueling cases are plotted).

Similarly robustness with respect to output unmodeled uncertainty is investigated. Opened loop system has two inputs pitch rate q and normal acceleration N_z (controller inputs) and two measurements of same notations (plant outputs). Nichols chards of open loop transfer functions are plotted in Figure 4.19 and its

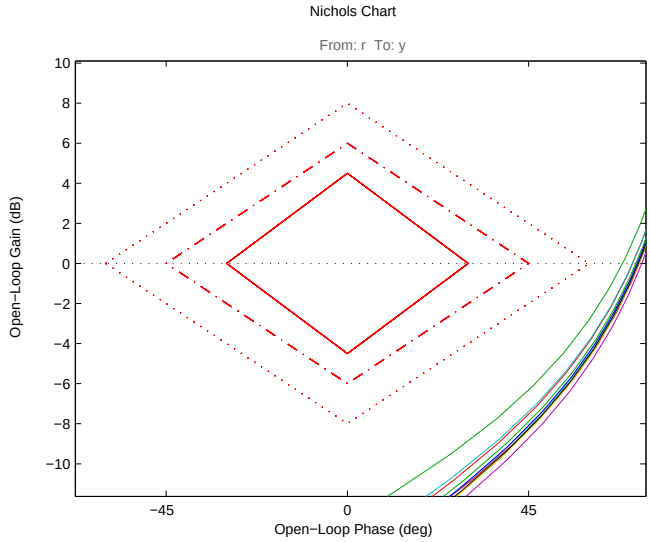

Figure 4.18: Nichols charts of closed loop disconnected at actuator, zoomed for Nichols diamonds (ten fueling cases are plotted).

zoom for Nichols diamonds are plotted in Figure 4.20.

Eventually Matlab Simuling nonlinear model has been involved. Main sources of nonlinearity come from fully nonlinear model of actuators, which consider control surface maximal deflection, maximal deflection rate and aerodynamic effects. All nonlinear simulation are influenced by unstable phugoid mode, but with time constant of unstability less than 0.1 seconds it does not violated control constrains or requirements. Time responses of aircraft normal acceleration for all considered aircraft fuel cases are plotted in Figure 4.21. The pitch rate and angle of attack responses are plotted in Figure 4.22 and 4.23, again plotted for all considered cases. Finally control law effort needed for such a maneuver, for all fuel cases, are plotted in Figure 4.24.

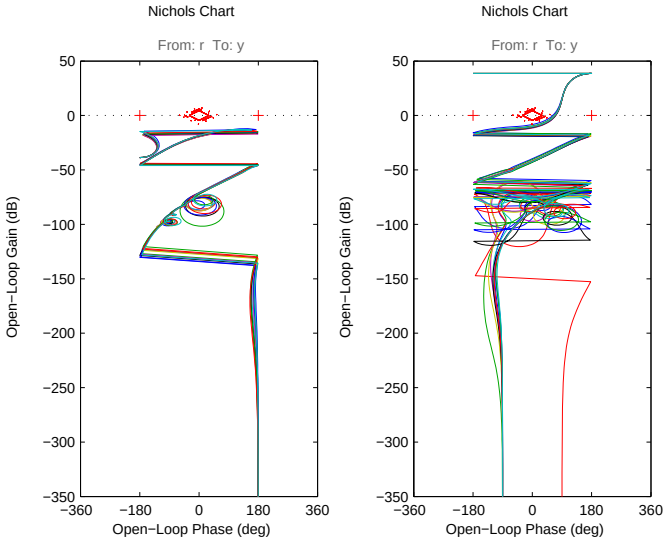

Figure 4.19: Nichols charts of closed loop disconnected at sensors, pitch rate (left) and Nz_{CG} (right). (ten fueling cases are plotted)

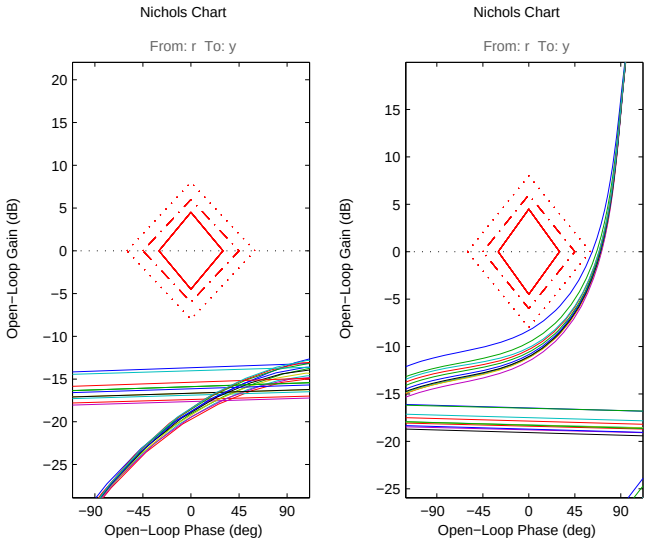

Figure 4.20: Nichols charts of closed loop disconnected at sensors, pitch rate (left) and Nz_{CG} (right), zoomed for Nichols diamonds (ten fueling cases are plotted).

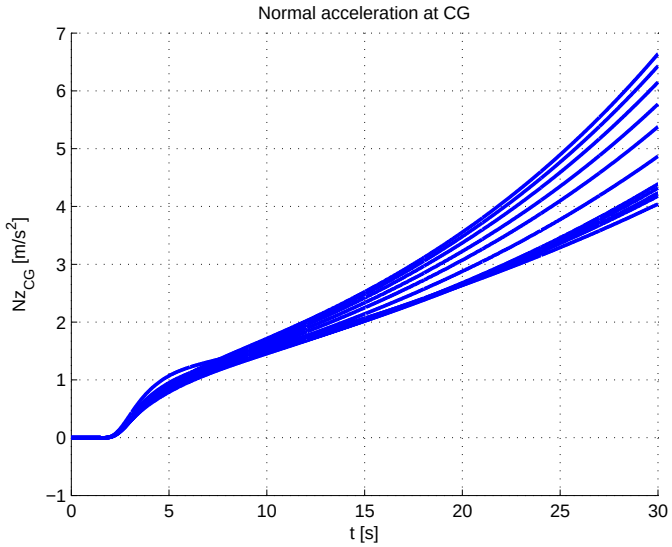

Figure 4.21: Normal acceleration step response (ten fueling cases are plotted).

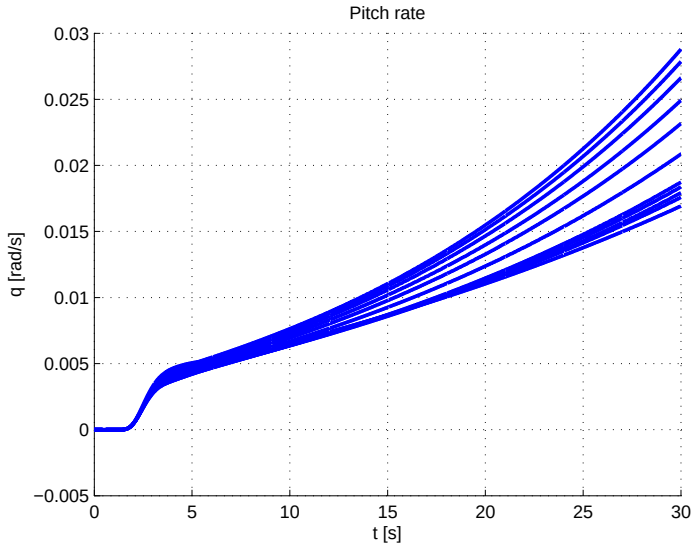

Figure 4.22: Pitch rate response to step in normal acceleration reference signal (ten fueling cases are plotted).

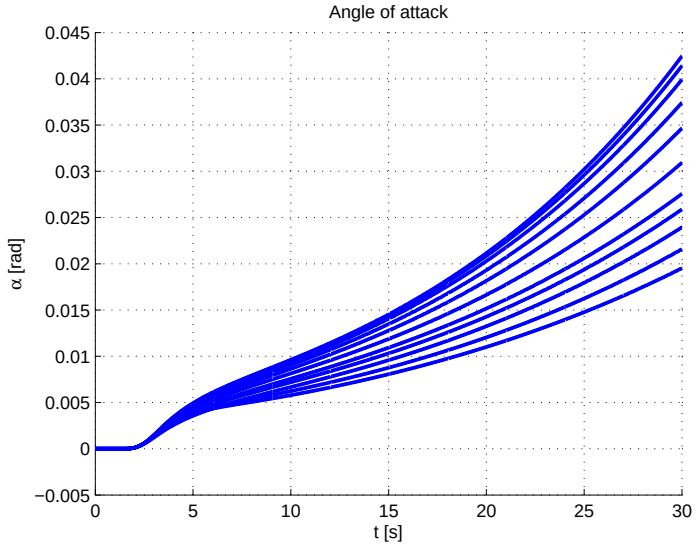

Figure 4.23: Angle of attack response to step in normal acceleration reference signal (ten fueling cases are plotted).

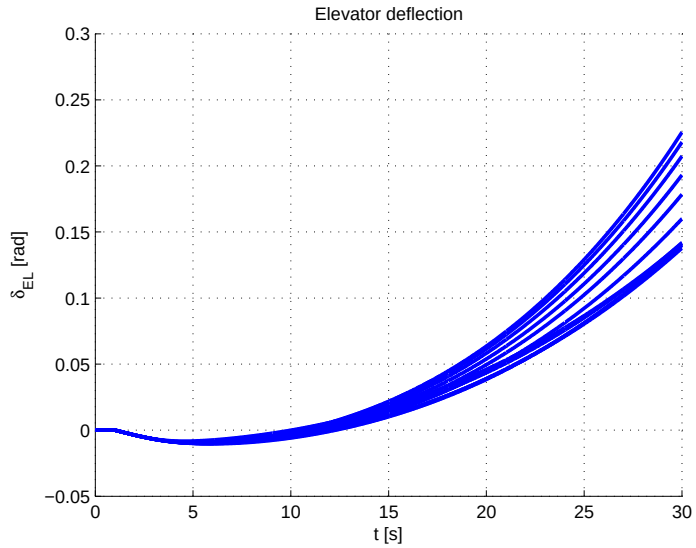

Figure 4.24: Elevator command required for step in normal acceleration reference signal tracking (ten fueling cases are plotted).

Chapter 5

Convex optimization design of feed-forward control for gust load alleviation

The potential advantages of Blended Wing Body (BWB) aircraft in terms of fuel efficiency are opposed by technical challenges such as the alleviation of gust loads. Due to the low wing loading gusts generally have a more severe impact on BWB aircraft than on conventional aircraft. This part presents the design and optimization of a Gust Load Alleviation System (GLAS) for a large BWB airliner. Numeric simulations are performed with an aeroelastic model of the aircraft including GLAS in order to compute time series of modal displacements for deriving equivalent static load cases which are used for resizing of the aircraft structure.

5.1 Introduction

For a significant fuel efficiency improvement on long-range transport aircraft, the transition to BWB (Blended Wing Body) configurations offers a promising long term solution. The advantage of higher lift to drag ratio is opposed by technical challenges such as the design of a flat pressurized cabin, specific demands on the

control system due to the high coupling between flap deflections and aircraft movements in all three axes. Due to the low wing loading BWB aircraft are generally more sensitive to gust loads than conventional wing tube aircraft. The investigations in this section are based on the BWB aircraft. The structural concept is based on gust and maneuver load computations. The coupled aeroelastic/flight mechanic BWB model used for this investigation is parameterized in Mach, dynamic pressure, fuel mass, and CG position. The CG variation is achieved by fuel redistribution which is important on a BWB airplane for trim without too large control surface deflections in order to achieve optimum cruise performance. For some fuel configurations the BWB airliner is statically unstable, thus requiring artificial stabilization. The BWB airliner is controlled/stabilized by underlying feedback control system using trailing edge flaps (design of feedback control law is not part of this section). The elevators flaps and spoilers on the upper side of the wings are used for feed-forward control. On each wing the 3 inner spoilers are actuated simultaneously, and the 3 outer spoilers are actuated simultaneously. The commands of the feed-forward gust load alleviation system are just added to the commands of feedback flight control law. Taking into account maneuver load alleviation, gust loads become the dominant sizing factor. For efficient gust load alleviation, the weighted L_∞ norm of the responses of wing bending and torsion moment need to be minimized for gusts of different scale lengths throughout the whole flight envelope while not exceeding maximum and minimum load factor. The worst case gust length of particular flight condition will be taken into account in this section, but augmentation of optimization for more gust length and operation points is strait forward and will by aim of future investigation.

5.2 Gust load alleviation system design

The Gust load alleviation system (GLAS) is based on triggered feed-forward control system for attenuation of aircraft excitation $\vec{d}(t)$ by exogenous disturbance signal $w(t)$, in our case wind gust of $1 - \cos$ shape. Design of the wind gust detection system, the trigger, is not considered in this paper. It is assumed that it is possible to estimate upcoming wind gust and its direction with certain time delay needed for estimation. Reference signal α_{wind} is than triggering signal used

as a input for GLAS feed-forward controller $H(s)$ and it is considered as a unit step signal. The GLAS $H(s)$ can be realized as a finite response filter (FIR) shaping input command α_{wind} and producing control signals $\vec{u}_{GLAS}$ or as a memory storing control signals $\vec{u}_{GLAS}$ and reading of memory is triggered by signal α_{wind}. The effect of $\vec{u}_{GLAS}$ on $\vec{e}(t)$ is expressed as a response of transfer function $G_c(s)$ so-called Secondary Control Path (SCP). Considering a model of the aircraft linearized in a certain trim point, the error signal $\vec{e}(t)$ is just the sum of aircraft response $\vec{d}(t)$ to wind gust disturbance $w(t)$ and response of the aircraft to GLAS control command $\vec{u}_{GLAS}$. The error signal $\vec{e}(t)$ contain wing bending and torsion moments as well as shear force at wing cut, as well as the incremental load factor $\Delta n_z(t)$. The design objective is to optimize $H(s)$ in order to minimize the L_∞ norm of a criteria based on forces and moments as will be explained later, keep $\Delta n_z(t)$ within certain limits (for passenger safety), and at the same time do not exceed certain limits for the L_∞ norm of $\vec{u}_{GLAS}(t)$, i.e. considering saturation of control surfaces. The control surfaces used for GLAS are elevator $u_{Elevator}$ and spoilers $u_{Spoiler}$. The vector of control commands $\vec{u}_{GLAS}(t)$ thus can be written as:

$$\vec{u}_{GLAS}(t) = [u_{Elevator},\ u_{Spoiler}] \tag{5.1}$$

Where $u_{Elevator}$ is elevator control command and $u_{Spoiler}$ denotes spoilers command.

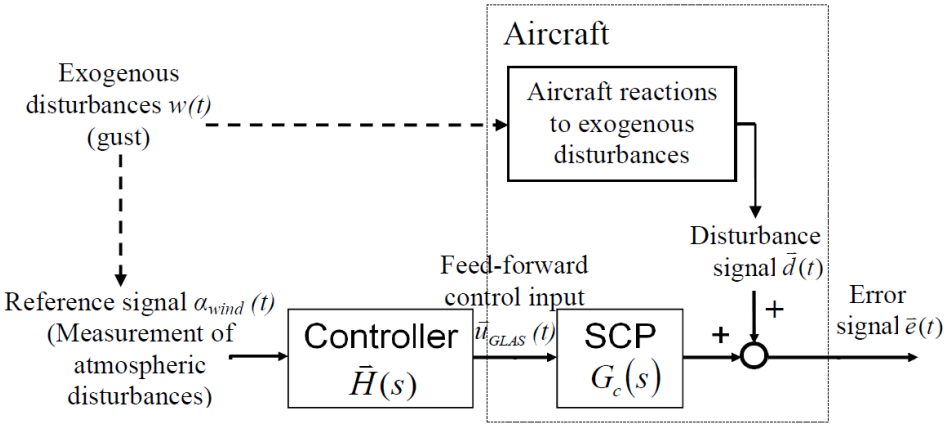

Figure 5.1: GLAS control setup

5.3 Convex synthesis

The convex synthesis approach is charged to design feed-forward control system. This methodology described by (Boyd et al., 1990*a*), (Boyd et al., 1990*b*), can easily address both time and frequency domain criterion and constraints. Nice overview and aircraft control system designed by convex synthesis was done in (Dardenne and Ferreres, 1998).

Let us consider generalized plant plotted in Figure 5.2. Where system P represents controlled plant, K is feedback control law and H is feed-forward control system. The signals w and z are exogenous input signals and controlled (criterion) output signals respectively. Signals u_{FF} and u_{FB} are input signal actuated by feed-forward and feedback control systems. The y and u_{REF} are measurable output signals and reference signal for feed-forward control system respectively.

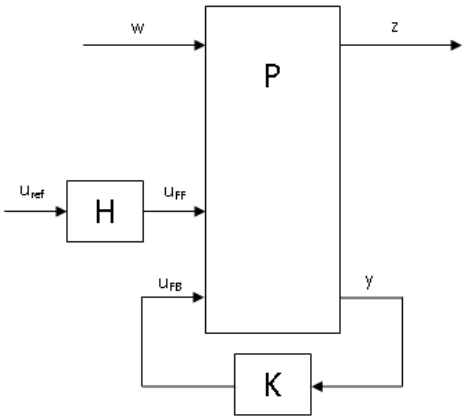

Figure 5.2: Convex synthesis plant

The convex synthesis methodology can be applied for both feedback and feed-forward control system design. Nevertheless only feed-forward control system design will be addressed in this section. Therefore the feedback control law K in Figure 5.2 is considered as a fixed control law. Then the parametrization of feed-forward controller $H(z)$ is done according to equation 5.2:

$$H(z) = \sum_{i=1}^{n} \theta_i \cdot H_i(z), \tag{5.2}$$

where the transfer functions $H_i(z)$ are a priory fixed basis functions and scalars θ_i for $i \leq 1$ are the decision variables of optimization problem. The exogenous input signal $w(t)$ is considered as one case of $1 - \cos$ shape gust (plotted in Figure 5.3). The result of optimization will be FIR filter $H(z)$ (decision variables θ_i defines coefficients of such a FIR filter), therefore the reference input signal u_{REF} is considered as a discrete impulse at time $t = 0$ plotted in Figure 5.4. The response of closed loop system can by expressed by equation 5.3 in a affine form:

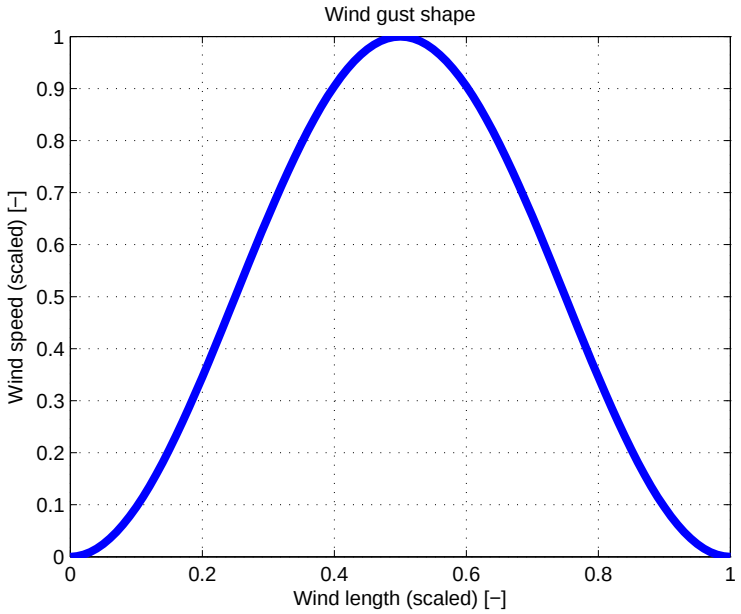

Figure 5.3: Wind gust shape.

$$z(t) = \theta_0 \cdot z_0(t) + \sum_{i=1}^{n} \theta_i \cdot z_i(t), \tag{5.3}$$

where $z_0(t)$ is response of closed loop system for disturbance signal $w(t)$ (according to equation 5.4, plotted in Figure 5.5), in this case coefficient θ_0 is equal to one. The second therm corresponds to the response of closed loop system (defined by equation 5.5, ploted in Figure 5.6 and Figure 5.7) for reference signal u_{REF} (in this case discrete impulse) shaped by particular basis function $H_i(z)$, in our case

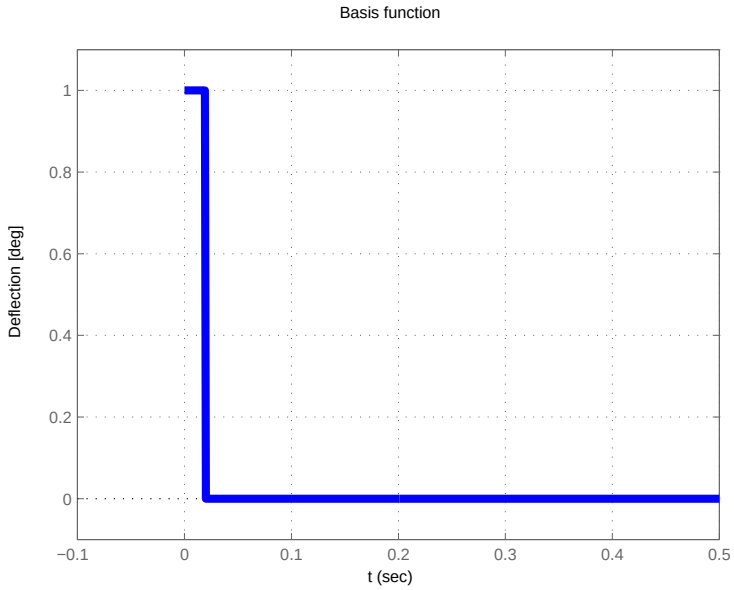

Figure 5.4: Reference input signal.

unit delay.

$$Z_0(z) = P(z) \cdot W(z) \tag{5.4}$$

$$Z_i(s) = P(z) \cdot H_i(z) \cdot U(z) \tag{5.5}$$

The correspondence between time and Z space is described by equation:

$$z_i(t) = Z^{-1} \left\{ Z_i(z) \right\}. \tag{5.6}$$

Eventually the convex optimization task can be defined as a linear program with criteria expressed as:

$$\min_{\theta} \left[c^T \cdot \theta \right], \tag{5.7}$$

and constraints:

$$A \cdot \theta \leq b \tag{5.8}$$

The criterion as well as constraints will be explained in details in section 5.4.

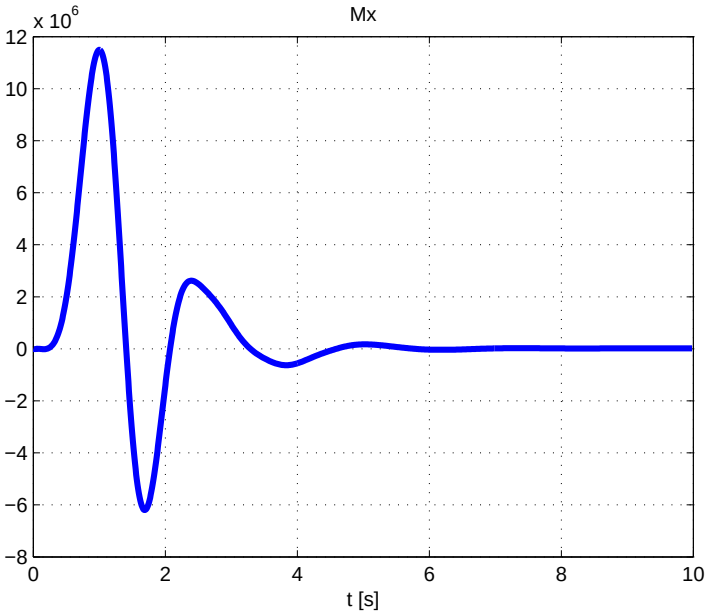

Figure 5.5: Mx response of Wind gust input.

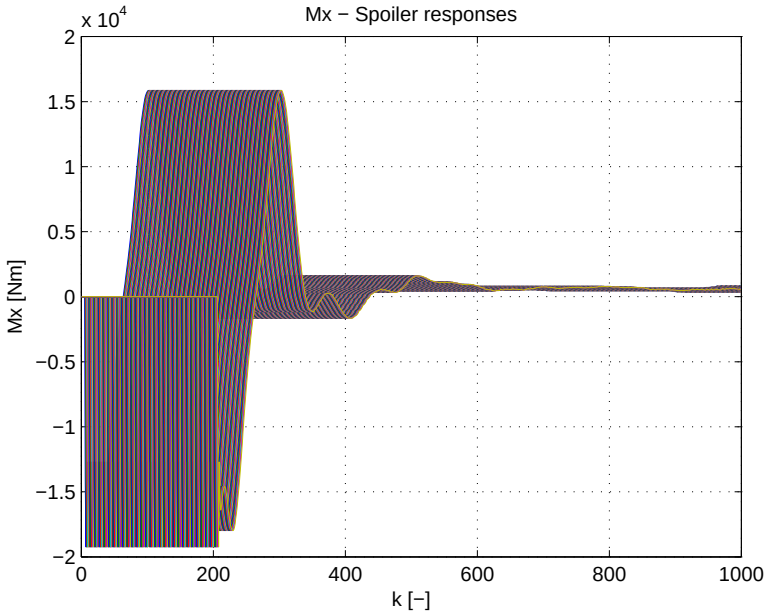

Figure 5.6: Mx responses of Spoiler input.

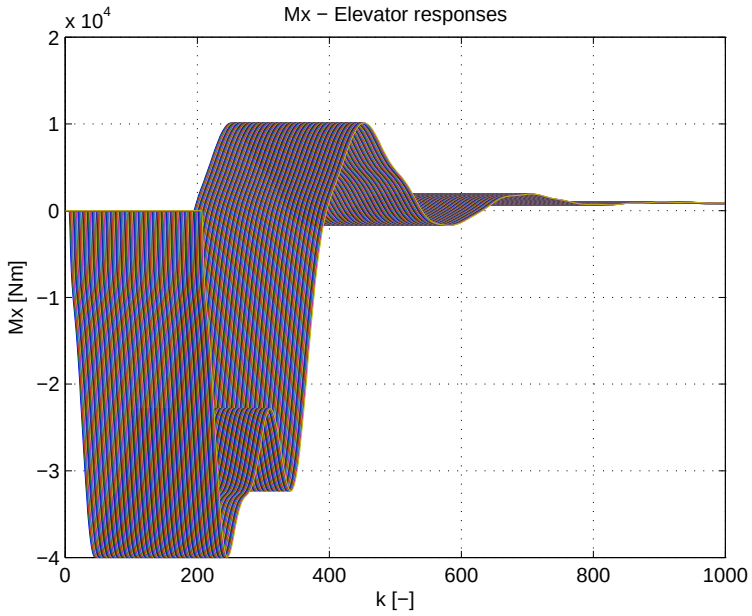

Figure 5.7: Mx responses of Elevator input.

5.4 Formulation of optimization problem

In the following the constraints for optimization of the time series of control commands for elevators and spoilers are formulated. With sizing gusts of different lengths from 30 feet to 500 feet starting at time $t = 0$ it was sufficient to fulfill following constraints within a time interval $[0; t_{end}]$ of 10 seconds since oscillations excited by gust diminish after that amount of time. First just one length of sizing wind gust case is considered to keep definition simple and clear. The maximum and minimum control surface deflections need to be bounded by:

$$u_{Elevator}(n) \leq u_{ElevatorMax}, \ \forall n \in [0; t_{end} \cdot F_s] \tag{5.9}$$

$$u_{Elevator}(n) \geq u_{ElevatorMin}, \ \forall n \in [0; t_{end} \cdot F_s] \tag{5.10}$$

$$u_{Spoiler}(n) \leq u_{SpoilerMax}, \ \forall n \in [0; t_{end} \cdot F_s] \tag{5.11}$$

$$u_{Spoiler}(n) \;\geq\; u_{SpoilerMin},\; \forall n \in [0; t_{end} \cdot F_s]\,. \tag{5.12}$$

With subscript *max* denoting maximum allowed deflection of the respective control surface, and subscript *min* denoting prescribed minimum allowed deflection of the respective control surface (maximal negative deflection). Control surface deflection rate $\frac{du}{dt}$ needs to be limited because the available actuators' energy is finite. Thereby, F_s is the sampling frequency, and $T_s = \frac{1}{F_s}$ denotes the sampling time of the discrete controller. Than rate limits of control surfaces are defined by:

$$\frac{u_{Elevator}(n) - u_{Elevator}(n-1)}{T_s} \;\leq\; \frac{du}{dt}_{ElevatorMax},\; \forall n \in [1; t_{end} \cdot F_s] \tag{5.13}$$

$$\frac{u_{Elevator}(n) - u_{Elevator}(n-1)}{T_s} \;\geq\; \frac{du}{dt}_{ElevatorMin},\; \forall n \in [1; t_{end} \cdot F_s] \tag{5.14}$$

$$\frac{u_{Spoiler}(n) - u_{Spoiler}(n-1)}{T_s} \;\leq\; \frac{du}{dt}_{SpoilerMax},\; \forall n \in [1; t_{end} \cdot F_s] \tag{5.15}$$

$$\frac{u_{Spoiler}(n) - u_{Spoiler}(n-1)}{T_s} \;\geq\; \frac{du}{dt}_{SpoilerMin},\; \forall n \in [1; t_{end} \cdot F_s] \tag{5.16}$$

For passenger safety, the maximum and the minimum load factor need to be bounded too.

$$n_z\,(n) \;\leq\; 2.5,\; \forall n \in [0; t_{end} \cdot F_s] \tag{5.17}$$

$$n_z\,(n) \;\geq\; 1,\; \forall n \in [0; t_{end} \cdot F_s]\,. \tag{5.18}$$

The cost function J is defined as a function of the vector of control commands $\vec{u}_{GLAS}(n)$ with tuning parameters a_1, a_2, a_3 and b_1, b_2, b_3. Considering that positive as well as negative peak force and moments needs to be reduced the cost function J can by divided into two parts:

$$
\begin{aligned}
J_{max} = \max_{n\in[0,\ t_{end}\cdot F_s]} & \Bigg[a_1 \cdot \Bigg(\sum_{i=0}^{n} f_z^{Gust}(i)\cdot w(n-i) + \sum_{i=0}^{n} f_z^{Elevator}(i)\cdot u_{Elevator}(n-i) \\
& + \sum_{i=0}^{n} f_z^{Spoiler}(i)\cdot u_{Spoiler}(n-i) \Bigg) \\
& + a_2 \cdot \Bigg(\sum_{i=0}^{n} m_x^{Gust}(i)\cdot w(n-i) + \sum_{i=0}^{n} m_x^{Elevator}(i)\cdot u_{Elevator}(n-i) \\
& + \sum_{i=0}^{n} m_x^{Spoiler}(i)\cdot u_{Spoiler}(n-i) \Bigg) \\
& + a_3 \cdot \Bigg(\sum_{i=0}^{n} m_y^{Gust}(i)\cdot w(n-i) + \sum_{i=0}^{n} m_y^{Elevator}(i)\cdot u_{Elevator}(n-i) \\
& + \sum_{i=0}^{n} m_y^{Spoiler}(i)\cdot u_{Spoiler}(n-i) \Bigg) \Bigg] \qquad (5.19)
\end{aligned}
$$

$$
\begin{aligned}
J_{min} = \min_{n\in[0,\ t_{end}\cdot F_s]} & \Bigg[b_1 \cdot \Bigg(\sum_{i=0}^{n} f_z^{Gust}(i)\cdot w(n-i) + \sum_{i=0}^{n} f_z^{Elevator}(i)\cdot u_{Elevator}(n-i) \\
& + \sum_{i=0}^{n} f_z^{Spoiler}(i)\cdot u_{Spoiler}(n-i) \Bigg) \\
& + b_2 \cdot \Bigg(\sum_{i=0}^{n} m_x^{Gust}(i)\cdot w(n-i) + \sum_{i=0}^{n} m_x^{Elevator}(i)\cdot u_{Elevator}(n-i) \\
& + \sum_{i=0}^{n} m_x^{Spoiler}(i)\cdot u_{Spoiler}(n-i) \Bigg) \\
& + b_3 \cdot \Bigg(\sum_{i=0}^{n} m_y^{Gust}(i)\cdot w(n-i) + \sum_{i=0}^{n} m_y^{Elevator}(i)\cdot u_{Elevator}(n-i) \\
& + \sum_{i=0}^{n} m_y^{Spoiler}(i)\cdot u_{Spoiler}(n-i) \Bigg) \Bigg] . \qquad (5.20)
\end{aligned}
$$

Finally overall criterion is defined as:

$$J = J_{max} - J_{min}. \tag{5.21}$$

Where, $w(n)$ is the discrete time gust excitation and $f_z^{Gust}(i)$, $f_z^{Elevator}(i)$, $f_z^{Spoiler}(i)$ denote the i^{th} sample of impulse responses of the linearised aircraft model to: gust excitation, elevators inputs and spoilers inputs. At same wing cut respective i^{th} sample of impulse responses for torsion moment are $m_y^{Gust}(i)$, $m_y^{Elevator}(i)$, $m_y^{Spoiler}(i)$, and for bending moment $m_x^{Gust}(i)$, $m_x^{Elevator}(i)$, $m_x^{Spoiler}(i)$. The static shear force, torsion moment and bending moment for $1g$ level flight are not considered in this paper. The optimization problem can thus be formulated as:

$$\min_{u_{Elevator},\ u_{Spoiler}} [J] \tag{5.22}$$

$$\tag{5.23}$$

With constraints expressed by equations 5.9, 5.10, 5.11, 5.12, 5.13, 5.14, 5.15, 5.16, 5.17 and 5.18.

5.5 Gust load alleviation system results

Simulations of resulting feed-forward control system are presented in this section. The deflections of spoilers and elevator commanded by triggered Gust Load Alleviation control system are plotted in Figure 5.8 and Figure 5.9. One can see that maximal and minimal deflection constraints of each control surface are fulfilled.

Similarly requirements for deflection rates of spoilers as well as elevators (plotted in Figures 5.10 and Figure 5.11) are take into account during optimization and fulfilled by resulting control law. One can see that deflection rate constraints are limiting factor of resulting control law and therefore achieved control law performance. The aircraft wing bending moment was reduced by more than 50% in sence of L_∞ norm. The resulting structural load aleviaton performance, due to bending of aircraft wing, is plotted in Figure 5.12.

Similarly the aircraft wing torsion moment was addressed and its value reduced by more than 60% in sence of L_∞ norm. The resulting structural load aleviaton

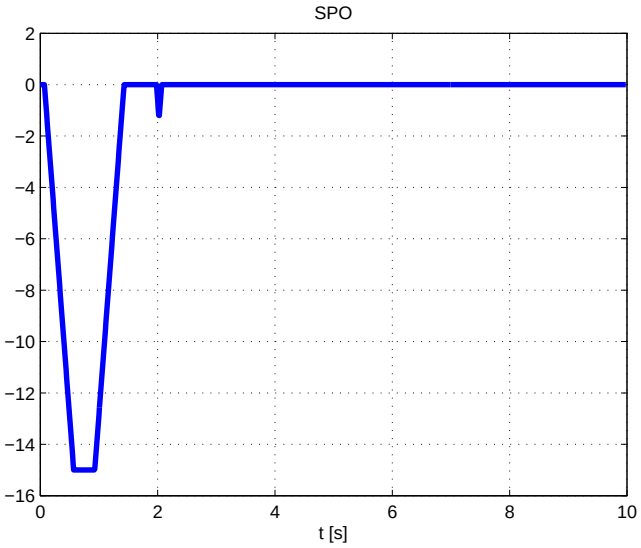

Figure 5.8: Spoiler deflection.

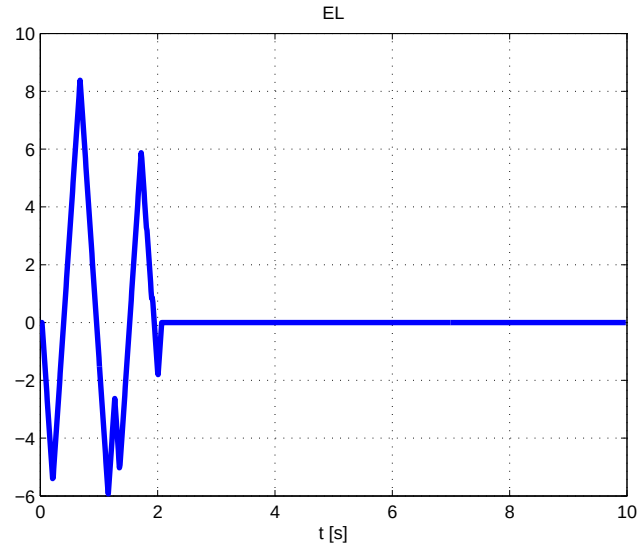

Figure 5.9: Elevator deflection.

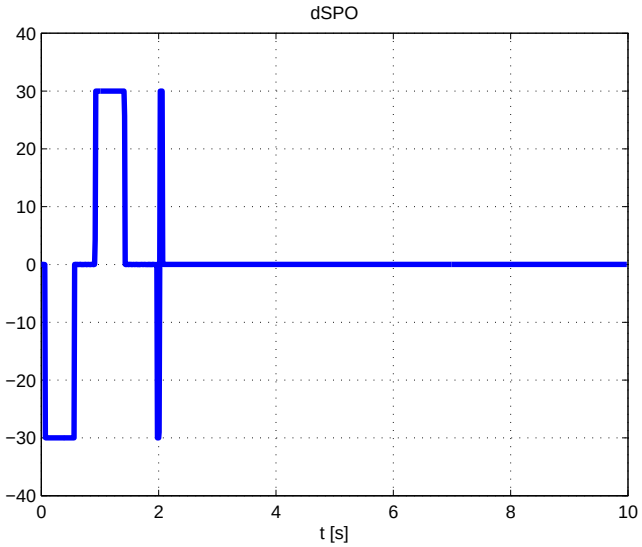

Figure 5.10: Spoiler deflection rate.

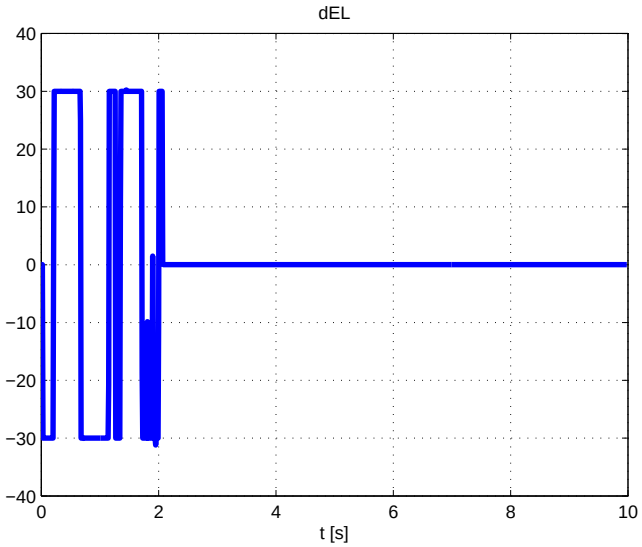

Figure 5.11: Elevator deflection rate.

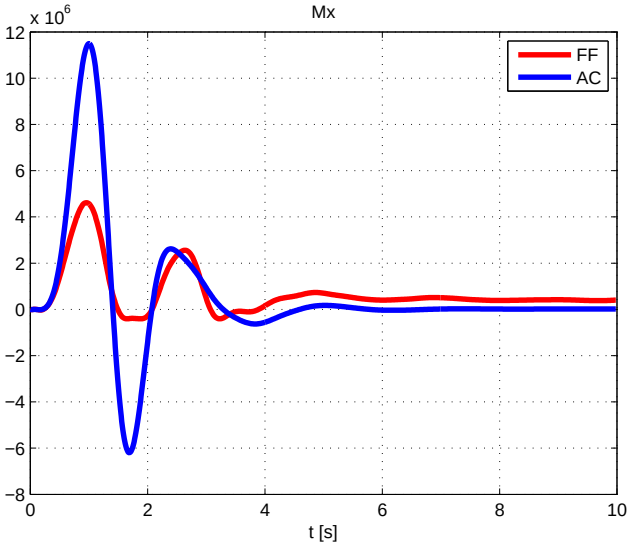

Figure 5.12: Bending moment attenuation.

performance, due to torsion of aircraft wing, is plotted in Figure 5.13. Eventually the vertical acceleration response is presented in Figure 5.14. One can see that also constrain for vertical acceleration is fulfilled.

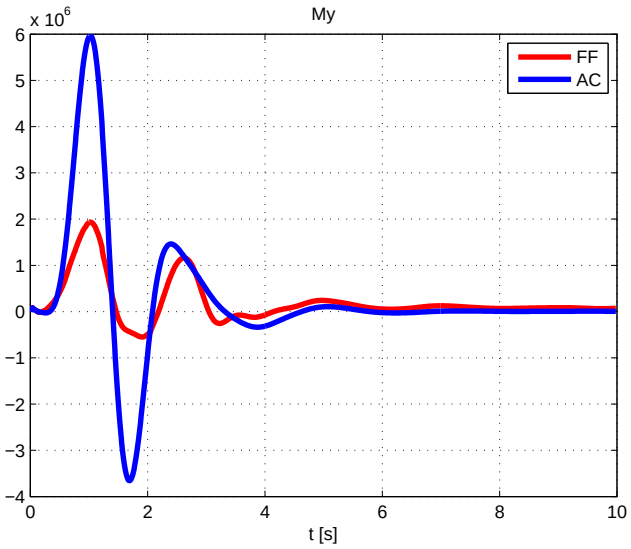

Figure 5.13: Torsion moment attenuation.

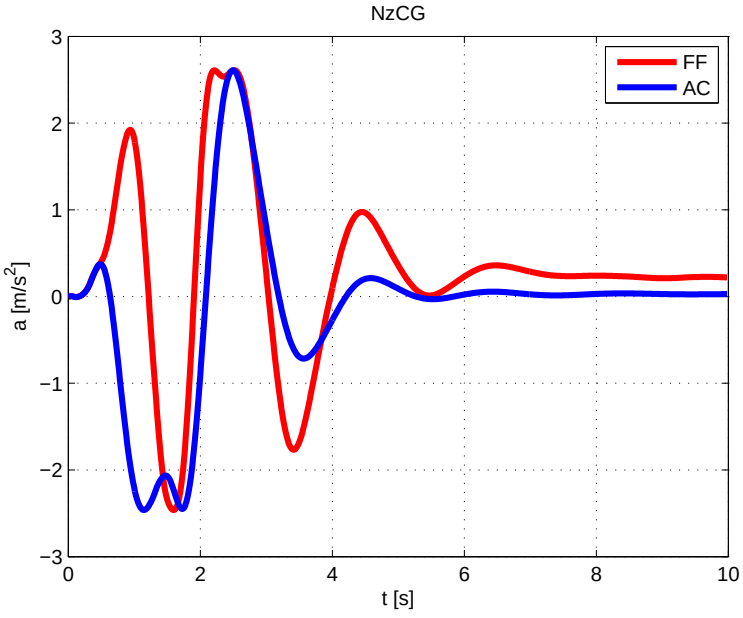

Figure 5.14: Vertical acceleration at center of gravity.

Chapter 6

Conclusion

The encapsulated methodology for flexible structure aircraft control design was presented in this thesis. First the novel approach to optimal sensors placement which takes into account the spillover issues has been presented in chapter 3. The information based approach was adopted, and a related effective algorithm was developed from the standard EFI procedure. Performance of the algorithm was assessed by meanings of a simple example and a Blended-Wing-Body aircraft case study.

The results of sensors positions optimization was one of the inputs for next part, the design of robust feedback control system presented in chapter 4. Lateral and longitudinal control system design were presented for both fully integrated flexible aircraft control system (rigid body and flexible modes are treated by one control law of low order) as well as rigid body motion control (where rigid body and flexible modes are treated by separate control laws).

Two efficient approaches to lateral control for the prospective BWB concept of large passenger aircraft are elaborated and assessed in section 4.1.3 and 4.3.1. First, a hierarchical approach is considered with separately designed control augmentation system (lateral autopilot with integrated beta-compensator and yaw damper) and the active damping system for structural vibrations on top of that. Main advantages of this approach are due to safety (the non-critical part - active damper - does not de-stabilize the plant if disengaged, e.g. due to a failure), easier

process of tuning and certification (step-by-step), and the results look very good in fact. On the other hand, this approach is conservative by its nature and does not exploit fully the potential of active control as a true MIMO overall controller could do. Therefore, the second approach also presented in the paper is a fully integrated H_∞ optimal control law of low order designed by fixed order optimization. Performance of both control strategies is assessed, and the integrated design indeed features better closed loop characteristics in terms of robustness (more mass cases covered), rise times, or Dutch-roll damping.

Finally the longitudinal flight control system of aircraft rigid body motions (again the aim of control law is handling of rigid body motion, but flexible modes are included in the model) was presented in section 4.4.2. The structure of control system was prescribed, in this case, and HiFOO toolbox is used to deliver H_∞ optimal control law fulfilling the requirements for structure, robustness and handling qualities. Performance of longitudinal flight control system is demonstrated by Blended Wing Body type aircraft case study in section 4.4.3.

The feed-forward flight control system was presented in the last part of this thesis (section 5). Where convex synthesis methodology was charged to deliver L_∞ optimal feed-forward control system. The aim of such a control system is alleviation of structural load induced by gust. Whether the gust induced load is usually sizing case of aircraft structure, the significant mass reduction would by possible due to usage of such a control system.

6.1 Main results

The goals of the thesis as prescribed in Chapter 2 were fulfilled in the following manner.

1. **Develop methodology for optimal sensor placement based on mathematical model of flexible aircraft structure.** Novel methodology for optimal sensor placement was delivered in chapter 3 based on Effective Independence Method. The EFI method, originally comes from buildings and structures monitoring optimization, was adopted and augmented by functionality of higher modes spillover suppression. The algorithm functionality

was first presented at ECC conference 2009, later on the results with BWB aircraft was presented at IFAC 2011 conference and in the journal paper [1] (accepted by the date of thesis submission).

2. **Deliver robust feedback control system methodology for aircraft with flexible structure based on modern optimization techniques.** The results in section 4 were logically divided into two parts, lateral and longitudinal control systems.

   (a) **Design of lateral Control Augmentation System (CAS) extended by the functionality of structural modes damper, but still of low complexity.** Two approaches for lateral CAS design are presented in section 4.1.3. First more tradition one approach provide H_2 optimal CAS based on frequency constrained LQ design technique. The control of flexible structure was designed by robust H_∞ optimization. The fully integrated CAS and flexible structure controller is presented in section 4.3.1. Where HiFOO toolbox was charged to deliver robust H_∞ optimal lateral control system of extremely low order. The comparison of resented approached was presented at IFAC 2011 conference.

   (b) **Longitudinal CAS design of flexible aircraft rigid body motions with prescribed structure.** The novel approach for lateral CAS system design is presented in section 4.4. Where HiFOO toolbox is employed to deliver longitudinal CAS system of low order, but in this case predefined structure of control law (adopted from conventional hierarchical control design methodology) is enforced. The advantages of hierarchical approach are preserved, but all drawback of loop by loop tuning approach are removed by usage of presented methodology. This approach was first presented at EUCASS 2011 conference and later on in journal paper [2](submitted by date of thesis submission).

3. **Design feed-forward load alleviation system for aircraft with flexible structure.** The feed-forward control system was introduced in section 5. The convex synthesis tool was used to develop triggered feed-forward structural gust load alleviation system. This part is main result of six month

intership at EADS Innovation Works in Munich. The results of this section were patented by EADS as European patent No. 11175857.9 - 1239 [4].

6.2 Suggestions for Future Research

The thesis raises some questions and problems that have not been answered yet. Namely:

- Full mathematical prove of information based and energy based approach equivalence. The direct comparison of those two approaches has been presented in the joint paper presented at Mathmod conference 2009 in Vienna. The simple textbook example was used to compare results of such a optimizations. The mathematical prove should unify both approaches.
- Augmentation / modification of OSP algorithm for non-oscillatory modes. The assumption of decoupled modes with low damping take account during optimization. This requirement is really limiting factor and determine using of this methodology.
- Implementation of genetic algorithm on top of HiFOO toolbox. This augmentation would introduce functionality of weighting filters generation.
- Optimal selection of input signals used for convex synthesis of load alleviation system. Convex optimization used for design of feed-forward control is limited by dimension of criteria (defined by sampling frequency and number of signals used for criteria or constrains definition) due to computational effort, therefore selection of criteria is really critical part of this approach.
- Design of feedback control system provide robustness of feed-forward load alleviation system.

These issues are now the subject of further research.

Bibliography

Aouf, N., Boulet, B. and Botez;, R. (2000), 'Robust gust load alleviation for a flexible aircraft', *Canadian Aeronautics and Space Journal* **46**, 131–139.

Apkarian, P. and Noll, D. (2006), 'Controller design via nonsmooth multidirectional search', *SIAM J. Control Optimization* **44**, 1923–1949.

Arzelier, D., Deaconu, G., Gumussoy, S. and Henrion, D. (2011), H2 for hifoo, *in* 'IFAC World Congress on Automatic control'.

Balas, G., Doyle, J. C. and Glover, A. (1991), *The mu analysis and synthesis toolbox*, Math Works and MUSYN.

Bates, D. and Postlethwaite, I. (2002), *Robust Multivariable Control of Aerospace Systems*, DUP Science.

Benatzky, C., Kozek, M., Schirrer, A. and Stribersky, A. (2008), Vibration damping of a flexible car body structure using piezo-stack actuators, *in* '17th IFAC WORLD CONGRESS'.

Bennami, S. and Looye, G. (1998), Design of flight control laws for a civil aircraft using mu sysnthesis, *in* 'Proc. of the AIAA Conference on Guidance, Navigation and Control'.

Blakelock, J. H. (1965), *Automatic Control of Aircraft and Missiles*, John Wiley & Sons.

Boyd, S., Barratt, C. and Norman, S. (1990*a*), *Linear controller design: limits of performance via convex optimization*, Prentice-Hall.

Boyd, S., Barratt, C. and Norman;, S. (1990*b*), 'Linear controller design: limits of performance via convex optimization', *Preoceedings of the IEEE* **78**, 529 – 574.

Brockhaus, R. (2001), *Flugregelung*, Springer.

Bryson, A. E. (1994), *Control of Spacecraft and Aircraft*, Princeton University Press.

Burke, J., Lewis, A. and Overton, M. (2005), A robust gradient sampling algorithm for nonsmooth, nonconvex optimization, *in* 'SIAM J. Optimization'.

Burke, J., Lewis, A. and Overton, M. (2006), 'Stabilization via nonsmooth, nonconvex optimization', *IEEE Transactions on Automatic Control* **51**, 1760–1769.

Burke, J. V., Henrion, D., Lewis, A. S. and Overton, M. L. (2006), Hifoo - a matlab package for fixed-order controller design and h-infinity optimization, *in* 'in IFAC Symposium on Robust Control Design'.

Chait, Y. and Radcliffet, C. J. (1989), 'Control of flexible structures with spillover using an augmented observer', *Journal of Guidance, Control, and Dynamics* **12**, 155–161.

Chang, C.-H. and Hant, K.-W. (1990), 'Gain margins and phase margins for control systems with adjustable parameters', *Journal of Guidance, Control, and Dynamics* **13**, 404–408.

Choi, J. W. and Park, U. S. (1989), 'Spillover stabilization of large space structures', *Journal of Guidance, Control, and Dynamics* **13**, 599–602.

Choi, J. W. and Park, U. S. (2001), 'Spillover suppression via eigenstructure assignment in large flexible structures', *Journal of Guidance, Control, and Dynamics* **20**, 599–602.

Chopra, I. and Ballardf, J. (1981), A method for measuring the stability of a full-scale rotor control system, *in* 'Journal of Guidance, Control, and Dynamics'.

Dardenne, I. and Ferreres, G. (1998), Design of a flight control system for a highly flexible aircraft using convex synthesis, *in* '21st Congress fo the International Council of the Aeronautical Sciences'.

Delwiche, T. (2009), Contribution to the Design of Control Laws for Bilateral Teleoperation with a View to Applications in Minimally Invasive Surgery, PhD thesis, Free University of Brussels.

Dotta, D., Silva, A. S. and Decker, I. C. (2009), Design of power systems controllers by nonsmooth, nonconvex optimization, *in* 'In IEEE Power and Energy Society General Meeting'.

Doyle, J. C. (1979), Robustness of multiloop linear feedback systems, *in* 'Proc. 17th IEEE Conf. Decision and Control'.

Doyle, J. C. (1982), Analysis of feedback systems with structured uncertainties, *in* 'IEE Proc.'.

Doyle, J. C., Glover, K., Khargonekar, P. and Francis, B. (1989), State space solutions to standard h2 and hinf control problems, *in* 'IEEE Trans. Aut. Control'.

Doyle, J. C., Mall, J. and Stein, G. (1982), Performance and robustness analysis for structured uncertainty, *in* 'IEEE Conf. on Decision and Control'.

Doyle, J. C. and Packard, A. (1987), Uncertain multivariable systems from a state space perspective, *in* 'Proc. of American Control Conference'.

Doyle, J. C., Packard, A. and Zhou, K. (1987), Review of lft's lmis and mu, *in* 'Proc. of 30th IEEE Conference on Decision and Control'.

Evans, W. R. (1948), 'Graphical analysis of control systems', *Trans. AIEE* **67**, 547–551.

Fialho, I., Balas, G., Packard, A., Renfrow, J. and Mullaney, C. (1997), Linear fractional transformation control of the f-14 aircraft lateral-direction axis during powered approach landing, *in* 'Proc. of the American Control Conference'.

Gawronski, W. (2004), *Advanced Structural Dynamics and Active Control of Structures*, Springer-Verlag.

Gumussoy, S., Henrion, D., Millstone, M. and Overton, M. (2009), Multiobjective robust control with hifoo 2.0, *in* 'IFAC Symposium on Robust Control Design'.

Gumussoy, S., Millstone, M. and Overton, M. (2008), H-infinity strong stabilization via hifoo, a package for fixed-order controller design, *in* 'in Proceedings of CDC'.

Gumussoy, S. and Overton, M. (2008), Fixed-order h-infinity controller design via hifoo, a specialized nonsmooth optimization package, *in* 'in Proceedings of ACC'.

Hanel, M. (2001), Robust integrated flight and aeroelastic control system design for a large transport aircraft, *in* 'Number 866 in 8. VDI-Verlag'.

Hansen, L. U., Heinze, W. and Horst, P. (2006), Representation of structural solutions in blended wing body preliminary design, *in* 'In 25th INTERNATIONAL CONGRESS OF THE AERONAUTICAL SCIENCES'.

Hyde, R. A. (1995), *Hinf Aerospace Control Design: A VSTOL Flight Application*, Springer Verlag.

Kammer, D. C. (1991), 'Sensor placement for on-orbit modal identification and correlation of large space structures', *Journal of Guidance, Control, and Dynamics* **14**, 251 – 259.

Kammer, D. C. (1992), 'Effect of model error on sensor placement for on-orbit modal identification of large space structures', *Journal of Guidance, Control, and Dynamics* **15**, 334–341.

Kammer, D. C. (1995), 'Optimal sensor placement for modal identification using system-realization methods', *Journal of Guidance, Control, and Dynamics* **19**, 729–731.

Kammer, D. C. (2005), 'Sensor set expansion for modal vibration testing', *Mechanical Systems and Signal Processing* **19**, 700 – 713.

Kammer, D. C. and Tinker, M. L. (2004), 'Optimal placement of triaxial accelerometers for modal vibration tests', *Mechanical Systems and Signal Processing* **18**, 29 – 41.

Kim, M.-H. and Inman, D. J. (2001), 'Reduction of observation spillover in vibration suppression using a sliding mode observer', *Journal of Vibration and Control* **7**, 1087–1105.

Knittel, D., Henrion, D., Millstone, M. and Vedrines, M. (2007), Fixed-order and structure h-infinity control with model based feedforward for elastic web winding systems, *in* 'in Proceedings of the IFAC/IFORS/IMACS/IFIP Symposium on Large Scale Systems'.

Kureemun, R. and Bates, D. G. (2001), Aircraft flight controls design using constrained output feedback - an h-infinity loopshaping approach, *in* 'AIAA Guidance, Navigation, and Control Conference'.

Lewis, A. and Overton, M. (2009), Nonsmooth optimization via bfgs, *in* 'SIAM J. Optimization'.

Lewis, F. (1986), *Optimal Estimation*, John Wiley & Sons.

Lewis, F. L. and Syrmos, V. L. (1995), *Optimal Control*, John Wiley & Sons.

Li, D., Li, H. and Fritzen, C. (2007), 'The connection between effective independence and modal kinetic energy methods for sensor placement', *Journal of Sound and Vibration* **305**, 945–955.

Liebeck, R. H. (2004), 'Design of the blended wing body subsonic transport', *Journal of Aircraft* **41**, 10 – 25.

Liu, W., Houand, Z. and Demetriou, M. A. (2006), 'A computational scheme for the optimal sensor/actuator placement of flexible structures using spatial h2 measures', *Mechanical Systems and Signal Processing* **20**, 881–895.

McFarlane, D., Glover, K., Khargonekar, P. and Francis, B. (1992), A loop-shaping design procedure using hinf synthesis, *in* 'IEEE Trans. Aut. Control'.

McRuer, D., Ashkenas, I. and Graha, D. (1973), *Aircraft Dynamics and Automatic Control*, Princeton University Press.

Meo, M. and Zumpano, G. (2005), 'On the optimal sensor placement techniques for a bridge structure', *Engineering Structures* **27**, 1488–1497.

Miller, J. E. (1966), *Space Navigation, Guidance and Control*, AGARDograph.

Millstone, M. (2006), Hifoo1.5: Structured control of linear systems with a non-trivial feedthrough, Master's thesis, Department of Mathematics, Courant Institute of Mathematical Sciences - New York University.

Perkins, C. D. (1970), 'Development of airplane stability and control', *Journal of Aicraft* **7**, 290–301.

Perng, B.-F. W. J.-W. (2004), 'Gainď and phase margin analysis of pilot-induced oscillations for limit-cycle prediction', *Journal of Guidance, Control, and Dynamics* **27**, 59–65.

Postlethwaite, I., Smerlas, A., Walker, A., Gubbels, A. W., Baillie, S., Strange, M. E. and Howitt, J. (1999), 'Hinf control of the nrc bell 205 fly-by-wire helicopter', *Journal of the American Helicopter Society* **44**, 276–284.

Poston, W. L. and Tolson, R. H. (1992), 'Maximizing the determinant of the information matrix with the effective independence method', *Journal of Guidance, Control, and Dynamics* **15**, 1513 – 1514.

Pouly, G., Lauffenburger, J.-P. and Basset, M. (2010), Reduced order hinfinity control design of a nose landing gear steering system, *in* '12th IFAC Symposium on Control in Transportation Systems'.

Qin, N., Vavalle, A., Moigne, A. L., Laban, M., Hackett, K. and Weinerfelt, P. (2004), 'Aerodynamic considerations of blended wing body aircraft', *Progress in Aerospace Sciences* **40**, 321–343.

Robu, B., Budinger, V., Baudouin, L., Prieur, C. and Arzelier, D. (2010), Simultaneous h-infinity vibration control of fluid/plate system via reduced-order controller, *in* 'Proceedings of CDC'.

Schirrer, A. (November 2011), Efficient robust control design and optimization methods for flight control, PhD thesis, Technical University of Vienna.

Schirrer, A., Westermayer, C., Hemedi, M. and Kozek, M. (2010*a*), Lq-based design of the inner loop lateral control for a large flexible bwb-type aircraft, *in* 'In 2010 IEEE Multi-Conf. on Systems and Control'.

Schirrer, A., Westermayer, C., Hemedi, M. and Kozek, M. (2010*b*), Robust hinf control design parameter optimization via genetic algorithm for lateral control of a bwb-type aircraft, *in* 'In IFAC Workshop on Intell. Control Systems'.

Schuler, J. (1997), Flugregelung und aktive Schwingungsdampfung fr flexible Groraumflugzeuge (engl. Flight control and active vibration damping for large flexible aircraft), PhD thesis, Universitt Stuttgart.

Skelton, R. E., Stoustrup, J. and Iwasaki, T. (2007), 'The hinf control problem using static output feedback', *International Journal of Robust and Nonlinear Control* **4**, 449–455.

Skogestad, S. and Postlethwaite, I. (1996), *Multivariable Feedback Control: Analysis and Design*, John Wiley & Sons.

Skogestad, S. and Postlethwaite, I. (2005), *Multivariable Feedback Control: Analysis and Design; 2nd edition*, John Wiley & Sons Ltd.

Stevens, B. L., Lewis, F. L. and Al-Sunni, F. (1992), 'Aircraft flight controls design using output feedback', *Journal of Guidance, Control, and Dynamics* **15**, 238–246.

Stevens, B. and Lewis, F. L. (2003), *Aircraft Control and Simulation*, John Wiley & Sons.

Stevens, B., Vesty, P., Heck, B. and Lewis, F. (1983), Loop shaping with output feedback, *in* 'American Control Conference'.

Torczon, V. (1991), On the convergence of the multidirectional search algorithm, *in* 'SIAM J. Optimization'.

Torczon, V. (1997), On the convergence of pattern search algorithms, *in* 'SIAM J. Optimization'.

Voskuijl, M., Rocca, G. L. and Dircken, F. (2008), Controllability of blended wing body aircraft, *in* 'In 25th INTERNATIONAL CONGRESS OF THE AERONAUTICAL SCIENCES'.

Wang, F. and Chen, H. (2009), 'Design and implementation of fixed-order robust controllers for a proton exchange membrane fuel cell system', *International Journal of Hydrogen Energy* **34**, 2705–2717.

Westermayer, C. (November 2011), 2DOF parameter-dependent longitudinal control of a blended wing body flexible aircraft, PhD thesis, Technical University of Vienna.

Westermayer, C., Schirrer, A., Hemedi, M. and Kozek, M. (2010), Linear parameter-varying control of a large blended wing body flexible aircraft, *in* 'In 18th IFAC Symposium on Automatic Control in Aerospace'.

Westermayer, C., Schirrer, A., Hemedi, M., Kozek, M. and Wildschek, A. (2009), Robust hinf flight and load control of a flexible aircraft using a 2dof multi-objective design, *in* 'In Proceedings of 2009 CACS International Automatic Control Conference'.

Whorton, M., Buschek, H. and Calise, A. J. (1996), 'Homotopy algorithm for fixed order mixed h2/hinf design', *Journal of Guidance, Control, and Dynamics* **19**, 1262–1269.

Yao, L., Sethares, W. and Kammer, D. (1992), Sensor placement for on-orbit modal identification of large spacestructure via a genetic algorithm, *in* 'Systems Engineering, 1992., IEEE International Conference on'.

Zhou, K., Doyle, J. and Glover, K. (1996), *Robust and optimal control*, Prentice Hall.

List of Author's Publications

Publications of the author related directly to the thesis

Journal Papers

[1] Haniš T. and Hromčík M.; Optimal sensors placement and spillover suppression, *Mechanical Systems and Signal Processing*, accepted (Impact factor 2011 is 1.762).

[2] Haniš T. and Hromčík M.; H_∞ structured fixed order optimization tools for flight controls design, *Journal of Guidance, Control, and Dynamics*, submitted (Impact factor 2011 is 1.070).

[3] Haniš T. and Hromčík M.; Flexible aircraft lateral control law of low order, *Czech aerospace Processing*, Prague, 2/2011.

Patent

[4] Wildschek A. and Haniš T.; Methods and apparatus for minimizing dynamic structural loads of an aircraft, *EADS - IW, European patent No. 11175857.9 - 1239*, Munich, 2011.

Conference Papers

[5] Haniš T. and Hromčík M.; Lateral Flight Dynamic Controller for Flexible BWB Aircraft; *Proceedings of the 18th International Conference on Process Control [CD-ROM]*. Bratislava: Slovenská technická univerzita, 2011, p. 333-337. ISBN 978-80-227-3517-9.

[6] Haniš T. and Hromčík M.; Lateral control for flexible BWB high-capacity passenger aircraft; *Proceedings of the 18th IFAC World Congress, 2011 [CD-ROM]*. Bologna: IFAC, 2011, p. 7233-7237. ISBN 978-3-902661-93-7.

[7] Haniš T. and Hromčík M.; Information-based sensor placement optimization for BWB aircraft; *Proceedings of the 18th IFAC World Congress, 2011 [CD-ROM]*. Bologna: IFAC, 2011, p. 2236-2241. ISBN 978-3-902661-93-7.

[8] Haniš T., Kučera and Hromčík M.; Low Order H infinity Optimal Control for ACFA Blended Wing Body; *4th European Conference for Aerospace Sciences [CD-ROM]*. SaintPetersburg: Eucass, 2011.

[9] Haniš T., Wildschek, A. and Stroscher, F.; Fuel Management System for Cruise Performance Optimization on a large Blended Wing Body Airliner; *4th European Conference for Aerospace Sciences [CD-ROM]*. SaintPetersburg: Eucass, 2011, p. 1-8.

[10] Haniš T., Wildschek, A. and Stroscher, F.; L infinity-Optimal Feed-forward Gust Load Alleviation Design for a large Blended Wing Body Airliner; *4th European Conference for Aerospace Sciences [CD-ROM]*. SaintPetersburg: Eucass, 2011 .

[11] Haniš T. and Hromčík M.; Optimal sensors placement and elimination of undesirable mode shapes; *European Control Conference 2009 - ECC 09 [CD-ROM]*. Budapest: MTA SZTAKI - Hungarian Academy of Sciences, 2009, p. 2045-2049. ISBN 978-963-311-369-1.

Publications of the author related indirectly to the thesis

Conference Papers

[12] Haniš T., Hromčík M.; Stabilized Platform for UAV; *Proceedings of the 8th International Scientific-Technical Conference Process Control 2008 [CD-ROM]*. Pardubice: University of Pardubice, 2008, p. 94. ISBN 978-80-7395-077-4.

[13] Řezáč, M., Žoha, J. and Haniš T.; Line-of-sight stabilization of an airborne camera system; *2008 PEGASUS-AIAA Student Conference [CD-ROM]*. Prague: Czech Technical University, 2008.

Vita

Tomáš Haniš was born on April 19, 1983 in Prague, Czech Republic. He got his Ing. degree (Czech equivalent to MSc.) in Technical Cybernetics, with major in control systems, at the Faculty of Electrical Engineering, Czech Technical University in Prague (FEE CTU), Czech Republic, in 2008. After graduation he got a position of a full time researcher at the Department of Control Engineering at FEE CTU. Tomáš Haniš is also involved in an bilateral project between FEE CTU and the Technical University in Vienna (Vienna, AT), focused on a design of optimal control strategies for transportation vehicles with flexible structures and European project ACFA 2020, focused on a design of optimal control system for advanced aircraft concepts. Teaching activities at FEE CTU cover labs of the Dynamics systems, Robust control, Flexible structure control and Flight control systems courses. He is supervising one diploma theses, two bachelor thesis and numerous of semestral projects.

Tomáš Haniš keeps contacts with leading universities and research institutes abroad. He has made several short-time visits to TUV (Vienna, Austria, fife stays), Utah State University and Space Dynamic Lab (Utah, USA, eight weeks). In addition, he spent six months at the EADS - Innovation works (Munich, Germany).

Tomáš Haniš is a student member of the American Institute of Aeronautics and Astronautics (AIAA) since 2008.

Tomáš Haniš presents his results regularly at prestigious international conferences including EUCASS, ECC and IFAC World Congress.

Address:

Department of Control Engineering,
Faculty of Electrical Engineering,
Czech Technical University in Prague
Karlovo náměstí 13/E,
121 35, Prague 2
Phone: +420 2 2435 7612, Fax: +420 2 2491 6648
E-mail: hanistom@fel.cvut.cz

This thesis was typeset with LaTeX 2_ε[1] by author.

[1] LaTeX 2_ε is an extension of LaTeXwhich is a collection of macros for TeX. TeX is a trademark of the American Mathematical Society.